HOXA5 Localization in Postnatal and Adult Mouse Brain Is Suggestive of Regulatory Roles in Postmitotic Neurons

Benoit Lizen, Bertrand Hutlet, Diane Bissen, Deborah Sauvegarde, Maryse Hermant, Marie-Thérèse Ahn, and Françoise Gofflot*

Institute of Life Sciences, Catholic University of Louvain, 1348 Louvain-la-Neuve, Belgium

ABSTRACT

Hoxa5 is a member of the *Hox* gene family, which plays critical roles in successive steps of the central nervous system formation during embryonic and fetal development. *Hoxa5* expression in the adult mouse brain has been reported, suggesting that this gene may be functionally required in the brain after birth. To provide further insight into the *Hoxa5* expression pattern and potential functions in the brain, we have characterized its neuroanatomical profile from embryonic stages to adulthood. While most *Hox* mapping studies have been based solely on transcript analysis, we extended our analysis to HOXA5 protein localization in adulthood using specific antibodies. Our results show that *Hoxa5* expression appears in the most caudal part of the hindbrain at fetal stages, where it is maintained until adulthood. In the medulla oblongata and pons, we detected *Hoxa5* expression in many precerebellar neurons and in several nuclei implicated in the control of autonomic functions. In these territories, the HOXA5 protein is present solely in neurons, specifically in γ-aminobutyric acid (GABA)ergic, glutamatergic, and catecholaminergic neurons. Finally, we also detected *Hoxa5* transcripts, but not the HOXA5 protein, in the thalamus and the cortex, from postnatal stages to adult stages, and in the cerebellum at adulthood. We provide evidence that some larger variants of *Hoxa5* transcripts are present in these territories. Our mapping analysis allowed us to build hypotheses regarding HOXA5 functions in the nervous system after birth, such as a potential role in the establishment and refinement/plasticity of precerebellar circuits during postnatal and adult life. J. Comp. Neurol. 525:1155–1175, 2017.

INDEXING TERMS: Hox gene; Hoxb5; Hoxc5; hindbrain; precerebellar nuclei; autonomous system; synaptic plasticity; noncoding transcripts; RRID: AB_262011; RRID: AB_2280649; RRID: AB_94647; RRID: AB_10601430; RRID: AB_2298772; RRID: AB_570666; RRID: AB_2187552; RRID: AB_10563603; RRID: AB_10564074; RRID: AB_2556546

The murine *Hoxa5* gene is a member of the *Hox* gene family coding for transcription factors that are key regulators of embryo patterning, organ development, and cell differentiation during animal development, but also adult life (Mallo et al., 2010; Rezsohazy et al., 2015). During development, *Hox* genes play critical roles in successive steps of central nervous system (CNS) formation, from neurulation to the establishment of functional neuronal networks (Nolte and Krumlauf, 2007; Dasen and Jessell, 2009; Narita and Rijli, 2009; Di Bonito et al., 2013a). Early in neurulation, the combinatorial expression of *Hox* genes provides segmental identity and anteroposterior patterning information to proliferating neural progenitors (Nolte and Krumlauf, 2007). After neurulation, *Hox* expression patterns are often maintained up to late fetal stages in restricted neuronal subpopulations (Oury et al., 2006; Pasqualetti et al., 2007; Geisen et al., 2008; Di Bonito et al., 2013b; Tomas-Roca et al., 2014). At these

Grant sponsor: Fonds de la Recherche Scientifique (FNRS); Grant number: MIS-Ulysse F.6003.09; Grant sponsor: Fonds Spéciaux de Recherche of the Université catholique de Louvain; Grant sponsor: Communauté française de Belgique-Actions de Recherche Concertées; Grant number: 12/17-041. B.L. is a FRIA fellow of the Fonds de la Recherche Scientifique.

Present address for D. Bissen: Max Planck Institute of Brain Research, Buchmann Institute of Molecular Life Sciences (BMLS), Frankfurt am Main, Germany

*CORRESPONDENCE TO: Françoise Gofflot, Institute of Life Sciences (ISV), Université catholique de Louvain, SST/ISV Carnoy, Croix du sud 4-5, bte L7.07.02, 1348 Louvain-la-Neuve, Belgium.
E-mail : Francoise.Gofflot@uclouvain.be.

Received February 16, 2016; Revised September 8, 2016;
Accepted September 15, 2016.
DOI 10.1002/cne.24123
Published online November 3, 2016 in Wiley Online Library (wileyonlinelibrary.com)

stages, *Hox* expression is notably required for normal tangential migration of pontine neurons, for proper axonal projection and arborization, for topographic connectivity, and for survival of neurons (Oury et al., 2006; Di Bonito et al., 2013b; Philippidou and Dasen, 2013; Bechara et al., 2015).

The evidence for an important role of *Hoxa5* in development comes mainly from the study of *Hoxa5* mutant mice. Depending on the genetic background, 50–80% of homozygous knockout (KO) pups die within 4 days of birth from respiratory distress, most probably caused by dysmorphogenesis of the respiratory tract (Aubin et al., 1997). Although *Hoxa5* is expressed in the developing spinal cord, where its anterior limit of expression corresponds to the posterior border of the myelencephalon (Nolte and Krumlauf, 2007), no alteration of the CNS was reported in the early studies of *Hoxa5* mutant mice. Indeed, the *Hoxa5* KO mice that survived until adulthood were fertile, with apparently normal behavior (Aubin et al., 1997, 1999, 2002). However, two recent reports have highlighted the expression and functions of *Hoxa5* at fetal stages in the spinal cord and more rostral CNS territories. First, within the spinal cord, Philippidou et al. (2012) showed that absence of *Hox5* genes (that is, *Hoxa5, Hoxb5*, and *Hoxc5*) resulted in a severe defect in diaphragm innervation and an important reduction and disorganization of motor neurons in the phrenic motor column. This defect could also contribute to the respiratory failure observed in $Hoxa5^{-/-}$ mutant mice (Philippidou et al., 2012). *Hoxa5* thus seems to be involved, together with other members of the paralogy group 5 (PG5) genes, in the clustering, intramuscular branching, and survival of neurons of the phrenic motor column. Second, although *Hoxa5* expression has not been reported in the hindbrain at early embryonic stages, it is detected in the posterior hindbrain at fetal stages, where it is involved in the tangential migration of precerebellar neurons from the rhombic lip toward the pontine gray nucleus (Di Meglio et al., 2013). The authors demonstrated that HOX5 proteins are functionally implicated in the topographic organization of migrating precerebellar pontine neurons, notably through the negative regulation of *Unc5b* expression, a netrin-repulsive receptor.

More recently, we have shown that *Hox* gene expression is maintained in the mouse brain at adulthood in territories derived from their early segmental expression domains in the hindbrain. Our data also revealed the presence of transcripts of *Hox* genes in territories where they have not been previously described during embryonic and fetal development, suggesting neoexpression in specific brain territories at adulthood (Hutlet et al., 2014). Strikingly, the relative abundance of *Hoxa5* transcripts measured by reverse transcriptase–qualitative polymerase chain reaction (RT–qPCR) in several brain subregions is similar to (e.g., in the cerebellum) or higher than (e.g., in the brainstem) the abundance measured in RNA extracted from embryos at different developmental stages, suggesting that *Hoxa5* expression is not trivial and could be functionally required in the brain after birth.

To complement these data and to fill in the gaps in what is understood about the dynamics of *Hoxa5* expression in the CNS, we undertook a spatiotemporal characterization of its expression pattern, at both RNA and protein levels, from embryonic stages to adulthood.

Abbreviations

AP	area postrema
Bfd	barrel field cortex
Cb	cerebellum
CNu	cerebral nuclei
Cx	cortex
CSC	cervical spinal cord
CU	cuneate nucleus
DMX	dorsal motor nucleus of the vagus nerve
ECU	external cuneate nucleus
GL	granular layer
HF	hippocampal formation
Hy	hypothalamus
GL	granular layer
GR	gracile nucleus
IF5	interfascicular trigeminal nucleus
IRN	intermediate reticular nucleus
KF	Kölliker–Fuse subnucleus
LGd	dorsal part of the lateral geniculate complex
LGv	ventral part of the lateral geniculate complex
LRN	lateral reticular nucleus
Mb	midbrain
MG	medial geniculate complex
MDRNd	dorsal part of the medullary reticular nucleus
ML	molecular layer
MO	medulla oblongata
MV	medial vestibular nucleus
NTS	nucleus of the solitary tract
OV	otic vesicle
P	pons
PARN	parvicellular reticular nucleus
PAS	parasolitary nucleus
PC	Purkinje cells
PG	pontine gray
PIR	piriform cortex
PRP	nucleus prepositus
PSV	principal sensory nucleus of the trigeminal
S	somite
SC	spinal cord
SPIV	spinal vestibular nucleus
SPVC	caudal part of the spinal nucleus of the trigeminal
SPVI	interpolar part of the spinal nucleus of the trigeminal
S3–S6	somites 3–6
Th	thalamus
TRN	tegmental reticular nucleus
WT	wild type
X	nucleus X
I–VI	cortical layers
Va	cortical layer 5a
XII	hypoglossal nucleus

Our analysis revealed that *Hoxa5* expression appears in the most caudal part of the hindbrain at fetal stages, where it is maintained until adulthood. In the hindbrain/medulla oblongata, *Hoxa5* expression is particularly enriched in precerebellar neurons, although it is also present in different nuclei implicated in the control of autonomic functions. In these territories, the HOXA5 protein is present specifically in γ-aminobutyric acid (GABA)ergic, glutamatergic, and catecholaminergic neurons. Finally, in agreement with our previous report, *Hoxa5* transcripts are also detected in forebrain territories, but only from postnatal stages onward. This mapping analysis allows the building of hypotheses about *Hoxa5* function in the nervous system after birth, and will thus serve as a stepping-stone for future functional studies.

MATERIALS AND METHODS

Animal and tissue processing

C57Bl/6J male and female mice (RRID: IM5R_JAX:000664), purchased from Charles River (Larbresle, France), were maintained in a conventional facility and fed a standard diet (rat/mice maintenance diet, Carfil Quality, Oud-Turnhout, Belgium) on a 14-hour light/10-hour dark cycle. Experimental procedures on animals were performed in accordance with the guidelines of the Animal Ethics Committee of the Université catholique de Louvain (approval 122803) and in agreement with European directive 2010/63/UE. For all gas euthanasia, CO_2 was administered by progressive delivery to the cage, with the volume in accordance with the guidelines.

For adult brain analyses, after a 4-hour fasting period, 12-week-old males were sacrificed by gas inhalation at 11–12 AM, and whole brains were rapidly isolated. For embryo and fetus recovery, pregnant females underwent gas euthanasia before dissection. The day of vaginal plug was considered as embryonic day (E)0.5, and embryos/fetuses were collected at several stages between E10.5 and E18.5. At postnatal stages, pups were sacrificed by gas inhalation, and whole brains were rapidly isolated. Embryos, fetus heads, and whole brains for in situ hybridization (ISH) were embedded in OCT mounting medium (Shandon Cryomatrix, Thermo Electron, Villebon sur Yvette, France), snap-frozen on dry ice, and stored at −80 °C. For RT-qPCR and western blot, adult brains were collected as described above, immediately dissected into eight subregions, frozen in liquid nitrogen, and stored at −80 °C. For immunohistochemistry (IHC) procedures, 12-week-old males were deeply anesthetized with an intraperitoneal lethal injection of sodium pentobarbital (Nembutal, CEVA, Sophia Antipolis,France; 80–100 mg/kg) and then rapidly perfused transcardially with phosphate-buffered saline (PBS, pH 7.4), followed by ice-cold 4% paraformaldehyde in PBS. After a last PBS wash, fixed brains were removed and cryopreserved in graded solutions of 10–20–30% sucrose in PBS at 4 °C (about 24 hours in each solution). Brains were embedded in OCT medium, frozen on dry ice, and stored at −80 °C. Embryos/fetuses were fixed in 4% paraformaldehyde in PBS for 15 minutes to 1 hour depending on the developmental stage and cryopreserved in 30% sucrose in PBS for several hours at 4 °C. E12.5 and older embryos were decapitated before fixation.

Gene expression studies: nonradioactive in situ hybridization

For ISH, 12 sets of 18-μm-thick serial coronal or sagittal cryosections per brain were cut on a Leica CM 3050S cryostat. Gene expression was detected using digoxigenin-labeled RNA probes, as previously described (Chotteau-Lelievre et al., 2006), and as optimized for *Hox* genes analysis in the adult brain (Hutlet et al., 2014).

Hoxa5 mRNA expression was detected with a probe transcribed from a 529-bp cDNA fragment containing nt 237–765, which specifically corresponds to *Hoxa5* gene exon 1 (Colberg-Poley et al., 1985). To detect only the longer *Hoxa5* transcripts, a probe of 603 bp corresponding to the *Hoxa5–Hoxa6* intergenic region was kindly provided by L. Jeannotte (Université Laval, Québec, Canada; probe b in Coulombe et al., 2010). The *Hoxb5* probe was transcribed from a 742-bp cDNA fragment overlapping exon 1 and exon 2 (Krumlauf et al., 1987), while the *Hoxc5* probe was transcribed from a 825-bp cDNA fragment overlapping exon 1 and exon 2 (Hutlet et al., 2014).

Gene expression studies: RT-qPCR

For the simultaneous isolation of RNA and proteins from the brain samples, the TRI Reagent product (T9424, Sigma-Aldrich, Machelen, Belgium) was selected. Brain subregions were homogenized in 1 ml of TRI Reagent for 30 seconds using a high-throughput tissue homogenizer (Precellys 24, Bertin Instruments, Montigny-le-Bretonneux, France). RNA was isolated from the dissected brain subregions following the manufacturer's instructions. The precipitated RNA pellet was dissolved in 100 μl of nuclease-free water, and reverse transcription was performed using a reverse transcription kit (Qiagen, 205311, Qiagen, Antwerpen, Belgium) according to the manufacturer's instructions. *Hoxa5* expression was assessed by qPCR on a StepOne + apparatus (Applied Biosystems, Ghent, Belgium) using SYBR Green as the detection method, and the geometric mean of two reference genes (*H2A* and *36B4*) as internal normalization reference. Normalized mRNA expression levels (means ± SEM from five mice) were reported as the mean value of *Hoxa5* in all brain samples.

TABLE 1.
Primers Used for Quantitative Polymerase Chain Reaction (qPCR)

Gene	Gene ID	Primer	5′ to 3′
Hoxa5	NM_010453	Hoxa5_qPCR-forward	gcgcaagctgcacattagt
		Hoxa5_qPCR-reverse	ggcatgagctatttcgatcc
H2A	NM_016750	H2A_qPCR-forward	gctggtggtggtgtcatcc
		H2A_qPCR-reverse	tttcttcccgatcagcgatt
36B4	NM_007475	36B4_qPCR-forward	tgagattcgggatatgctgttg
		36B4_qPCR-reverse	ttccaatggtgcctctggaga

The resulting relative expression levels were obtained by the ΔΔCQ method (see Table 1 for primer sequences).

Protein localization studies: immunohistochemistry

For IHC, 18-μm-thick serial cryosections were cut as above. After washes in TBS-Tx (Tris-buffered saline 0.05 M/Triton X-100 1%, pH 7.4), sections were blocked in a solution of 5% milk (Regilait 0% skim milk, Saint-Martin-Belle-Roche, France) in TBS-Tx (1 hour at room temperature [RT]). Sections were incubated overnight at 4 °C with primary antibody solution (antibody diluted in TBS-Tx 1% skim milk) in a humid chamber. After incubation with primary antibody, sections were rinsed with TBS-Tx and incubated for 1 hour at RT with the appropriate secondary antibody (1:500 in TBS-Tx 1% milk). After TBS-Tx washes, sections were stained with TB–4′6-diamidino-2-phenylindole [DAPI]; 1:20,000 for 10 minutes), and then mounted with Fluorescence Mounting Medium (Dako, Leuven, Belgium). The immunostained samples were examined with an Axioskop2 fluorescence microscope (Zeiss Instruments), and images were acquired on a Zeiss LSM 710 confocal microscope.

Protein localization studies: western blotting

After homogenization in TRI Reagent as described above, proteins were isolated from adult brain samples following the manufacturer's instructions, and the pellet was dissolved in sodium dodecyl sulfate (SDS) 1%/urea 8 M (v/v). Protein concentration was determined with a BCA protein assay (Pierce, Rockford, IL). Thirty μg of total soluble protein was loaded per lane on a 15% acrylamide SDS–polyacrylamide gel electrophoresis (SDS-PAGE). After transfer, the nitrocellulose membranes were blocked in 5% nonfat dry milk in TTBS (150 mM NaCl, 20 mM Tris, pH 7.5, with 0.1% Tween) at RT for 1 hour and then incubated in the primary antibody solution (TTBS, 1% milk, 0.05% sodium azide) overnight (see Table 2 for antibody information and dilution). Blots were washed in TTBS, followed by incubation with horseradish peroxidase (HRP)-conjugated secondary antibody (Dako, Carpinteria, CA) for 1 hour. Blots were developed with the Western Lightning Chemiluminescence kit (PerkinElmer, Oak Brook, IL) according to the manufacturer's instructions.

Antibody characterization

All primary antibodies used in this study are described in Table 2. To increase the robustness of our data, two anti-HOXA5 antibodies were used. Because results with these antibodies have not previously been published, we

TABLE 2.
Primary Antibodies Used in This Study

Antigen	Immunogen	Source	Dilution
β-ACTIN	Recombinant protein corresponding to amino acids 2–15 of mouse β-Actin	Mouse monoclonal Sigma-Aldrich cat# A3854, RRID: AB_262011	1:20,000 (WB)
CD11b/CD18 (Mac1)	T-cell–enriched splenocytes from B10 mice	Rat monoclonal Millipore cat# MAB1387Z, RRID: AB_2280649	1:200 (IF)
ChAT	Choline acetyltransferase purified from rat brain	Mouse monoclonal Millipore cat# MAB305, RRID: AB_94647	1:70 (IF)
GFAP	Bovine glial fibrillary acidic protein	Rat monoclonal Calbiochem cat# 345860	1:200 (IF)
HOXA5	Recombinant protein corresponding to amino acids 40–189 of human HOXA5	Rabbit polyclonal Sigma-Aldrich cat# HPA029319, RRID: AB_10601430	1:200 (IF) 1:500 (WB)
HOXA5	Synthetic peptide corresponding to amino acids 83–92 (EPRYSQPATS) of mouse HOXA5	Goat polyclonal antibodies-online.com cat# ABIN1590003	1:100 (IF)
NEUN	Purified cell nuclei from mouse brain	Mouse monoclonal Millipore cat# MAB377, RRID: AB_2298772	1:500 (IF)
OLIG2	Recombinant mouse Olig2	Rabbit monoclonal Millipore cat# AB9610, RRID: AB_570666	1:1,000 (IF)
TH	Tyrosine hydroxylase purified from PC12 cells	Mouse monoclonal Millipore cat# MAB318, RRID: AB_2201528	1:500 (IF)
VGLUT2	Recombinant protein from rat vesicular glutamate transporter 2	Mouse monoclonal Millipore cat# MAB5504, RRID: AB_2187552	1:100 (IF)

Abbreviations: IF, immunofluorescence; WB, western blot;

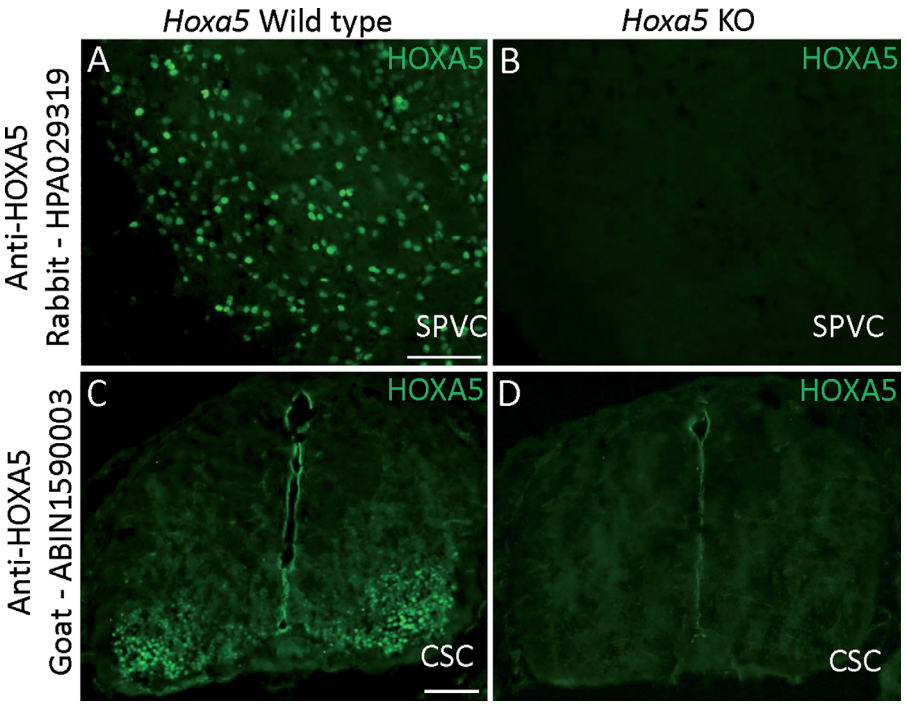

Figure 1. Specificity control for the two anti-HOXA5 antibodies used in this study. Immunolabeling of HOXA5 (green) on coronal cryosections of adult mouse brain using anti-HOXA5 (SIGMA HPA029319) (**A,B**) and on transversal cryosections of cervical spinal cord (CSC) of E12.5 embryo using anti-HOXA5 (antibodies-online.com ABIN1590003) (**C,D**). **A,C**: In the *Hoxa5* wild-type individuals, intense signal was observed (A) in the caudal part of the spinal nucleus of the trigeminal nerve (SPVC) and (C) in CSC of the E12.5 embryo. **B,D**: In the *Hoxa5* knockout, no signal was visible either in SPVC (B) or in CSC of E12.5 embryo (D). For abbreviations, see list. Scale bar = 50 μm in C (applies to A–D). [Color figure can be viewed at wileyonlinelibrary.com]

validated their specificity in IHC using tissues from *Hoxa5* KO embryos and adult brains (provided by L. Jeannotte, Université Laval, Québec, Canada; Aubin et al., 1997). Immunolabeling with the anti-HOXA5 antibody produced in rabbit (Sigma-Aldrich cat# HPA029319, RRID: AB_10601430) showed an intense signal on wild-type brain tissues and embryos while no signal was observed in the KO tissues, as illustrated in the caudal part of the spinal nucleus of the trigeminal nerve (SPVc) in the brain (Fig. 1A,B). Immunolabeling with the anti-HOXA5 antibody produced in goat (antibodies-online.com, cat# ABIN1590003) showed an intense signal on wild-type embryos and brains while no signal was observed in the KO embryos, as illustrated in the cervical spinal cord (CSC) at E12.5 (Fig. 1C,D). Other primary antibodies used in this study have previously been used in published studies (Goemaere and Knoops, 2012). The monoclonal mouse anti-neuronal nuclei (NEUN) antibody (Millipore, Billerica, MA, cat# MAB377, RRID: AB_2298772) gave a strong signal in most neuronal nuclei, although some specific neurons, for example, cerebellar Purkinje cells, did not show any signal for NEUN (Mullen et al., 1992). The OLIG2 rabbit polyclonal antibody (Millipore, cat# AB9610, RRID: AB_570666) was used to specifically stain the oligodendrocyte lineage (Zhou et al., 2000). The rat monoclonal anti-glial fibrillary acidic protein (GFAP) (Calbiochem, EMD Millipore, cat# 345860) was used as an astrocyte marker (Lee et al., 1984). CD11b/CD18 (macrophage antigen complex 1, Mac1) rat monoclonal antibody (clone M1/70; Millipore, cat# MAB13872 RRID: AB_2280649) labels a heterodimer (Springer, 1981; Sanchez-Madrid et al., 1983) corresponding to the αM integrin chain (165–170 kDa, CD11b) and the β2 integrin (95 kDa, CD18) which is expressed by mononuclear phagocytes, including microglia and granulocytes. In mouse brain this antibody was used as a microglial marker. Tyrosine hydroxylase (TH) mouse monoclonal antibody (Millipore, cat# MAB318, RRID: AB_2201528) was used to stain catecholaminergic (dopaminergic and noradrenergic) neuron populations (Masserano and Weiner, 1983). The vesicular glutamate transporter 2 (VGLUT2) mouse monoclonal antibody (Millipore, cat# MAB5504, RRID: AB_2187552) and the choline acetyltransferase (ChAT) mouse monoclonal antibody (Millipore, cat# MAB305, RRID: AB_94647) gave a signal with a distribution and a cellular pattern similar to those observed in previous publications (Cavicchioli et al., 1991; Vigneault et al., 2015).

Secondary antibodies used were as follows: Alexa Fluor 546 goat anti-rat IgG (H+L) (1:500, Thermo Fisher Scientific, Waltham, MA, cat# A1108, RRID: AB_10563603), Alexa Fluor 488 donkey anti-goat igG (H+L) (1:500, Thermo Fisher, cat# A11055 RRID: AB_10564074), Alexa Fluor 488 donkey anti-rabbit IgG (H+L) (1:500, Thermo Fisher, cat# R37118, RRID: AB_2556546), polyclonal goat anti-rabbit immunoglobulins/HRP (1:2,000, Dako, cat# P0448). Background labeling arising from the secondary antibodies was tested and considered not significant.

RESULTS

Dynamic expression of *Hoxa5* in the brain from embryonic to postnatal stages

As one of the PG5 genes, *Hoxa5* expression in the CNS during embryonic development (E9–E10.5) is known to be limited to the spinal cord, with an anterior border of expression located in the cervical region (Joksimovic et al., 2005; Nolte and Krumlauf, 2007). However, *Hoxa5* expression was recently reported in the adult brain, in territories derived from the hindbrain and forebrain (Hutlet et al., 2014). To provide further insight into this adult pattern, we first investigated how and when *Hoxa5* expression appeared in these territories, using ISH at different developmental and postnatal stages. At E10.5, we detected signal in the CNS with an anterior limit located in the spinal cord, facing somite 3 (Fig. 2A), as previously described (Joksimovic et al., 2005). At E12.5, the signal was maintained in the spinal cord, but labeling was also present in the caudal part of the hindbrain, extending rostrally over the cervical flexure (Fig. 2B). This expression domain in the caudal hindbrain remained unchanged until E14.5 (Fig. 2C). However, at E16.5, a few labeled cells were also observed in the ventral region of the anterior hindbrain, at the level of the pontine flexure (red arrow in Fig. 2D). This pattern, including the expression in the caudal hindbrain and the pons region, was stable until birth. After birth, expression of *Hoxa5* was maintained in these regions with no apparent changes in cellular pattern or intensity levels (Fig. 2E–J). In the cerebellum, we did not detect signal during postnatal stages (Fig. 2K–M). At postnatal day 12 (P12), a faint and scattered signal was first observed in several nuclei of the thalamus, mainly visible in the lateral geniculate nucleus (Fig. 2O). This signal was maintained through later stages (Fig. 2P) until adulthood. From P18, a signal was also detectable in the cortex (Fig. 2Q–S). This signal always appeared weaker than the signal detected in the caudal hindbrain of the same individual, and was observed in a few scattered cells located in a medial layer of the somatosensory cortex and in layer II of the piriform and entorhinal cortices.

Hoxa5 expression in the adult mouse brain

To gain insight into the later functions of *Hoxa5* in the brain, we next analyzed in detail the anatomical localization of *Hoxa5* transcripts in the adult mouse brain by ISH. For this systematic analysis, *Hoxa5* mRNA expression was detected with a probe transcribed from a 529-bp cDNA fragment containing nt 237–765, which specifically corresponds to the first (exon 1) of the two exons of the *Hoxa5* gene (Colberg-Poley et al., 1985). This probe thus detects the short 1.8-kb transcript that was shown to be translated in the HOXA5 protein (Coulombe et al., 2010). However, the use of multiple promoters and alternative splicing at the *Hoxa5* locus results in the production of larger transcript variants that all contain the two *Hoxa5* exons, and are thus also detected by our probe (see below). The signal described in this section thus corresponds to all the transcripts belonging to the *Hoxa5* transcriptional unit, including noncoding transcripts, independently of their potential to produce the HOXA5 protein.

Hindbrain

In sagittal section, a boundary was observed between a caudal territory in the medulla oblongata where labeling was widespread, and an anterior territory where signal was restricted to a few nuclei (data not shown). Dorsally, this boundary was located at the anterior limit of the area postrema (AP) corresponding to the enlarged 8th rhombomere. In the dorsolateral regions, *Hoxa5* signal was both stronger and more widespread than in the ventral part, where the signal was more scattered. On coronal sections, we identified 19 nuclei in the medulla oblongata in which *Hoxa5* transcripts were detected reproducibly at a high level ($n = 19$ brains; Fig. 3A–E,G, Table 3). While in some nuclei the signal was scattered, with only a fraction of cells labeled (e.g., MDRN), or patchy, with some cells appearing more labeled than others (e.g., SPVI; Fig. 3D), in other nuclei the signal appeared more homogenous, with a larger number of cells being labeled (e.g., AP; Fig. 3B). In addition to the medullar nuclei, labeling was also observed reproducibly in four nuclei in the pons (Fig. 3H–J, Table 3).

Strikingly, among the 23 nuclei labeled in the hindbrain, 18 were precerebellar nuclei, gathering neurons that project to the cerebellar cortex. By providing the main afferents to the cerebellum, these nuclei are essential for coordinated motor activity, motor learning, and procedural memory. The majority of the precerebellar nuclei give rise to mossy fibers (Rodriguez and Dymecki, 2000; Fu et al., 2013) that synapse with cerebellar granule cells. Among the nuclei in which we detected *Hoxa5* labeling were the pontine gray (PG), the tegmental reticular nucleus (TRN; Fig. 2I), the external cuneate nucleus (ECU; Fig. 3B,E), the lateral reticular nucleus (LRN; Fig. 3C), the interfascicular trigeminal nucleus (IF5; Fig. 3J), and the nucleus prepositus (PRP; Fig. 3E). These nuclei are referred to as the "major" precerebellar nuclei because they provide inputs almost exclusively to the cerebellum. In addition, we detected *Hoxa5* labeling in scattered cells of the cuneate nucleus (CU; Fig. 3B), nucleus x (X; Fig. 3G), the spinal nucleus of the trigeminal (SPV; Fig. 3A,D), and the Kölliker–Fuse

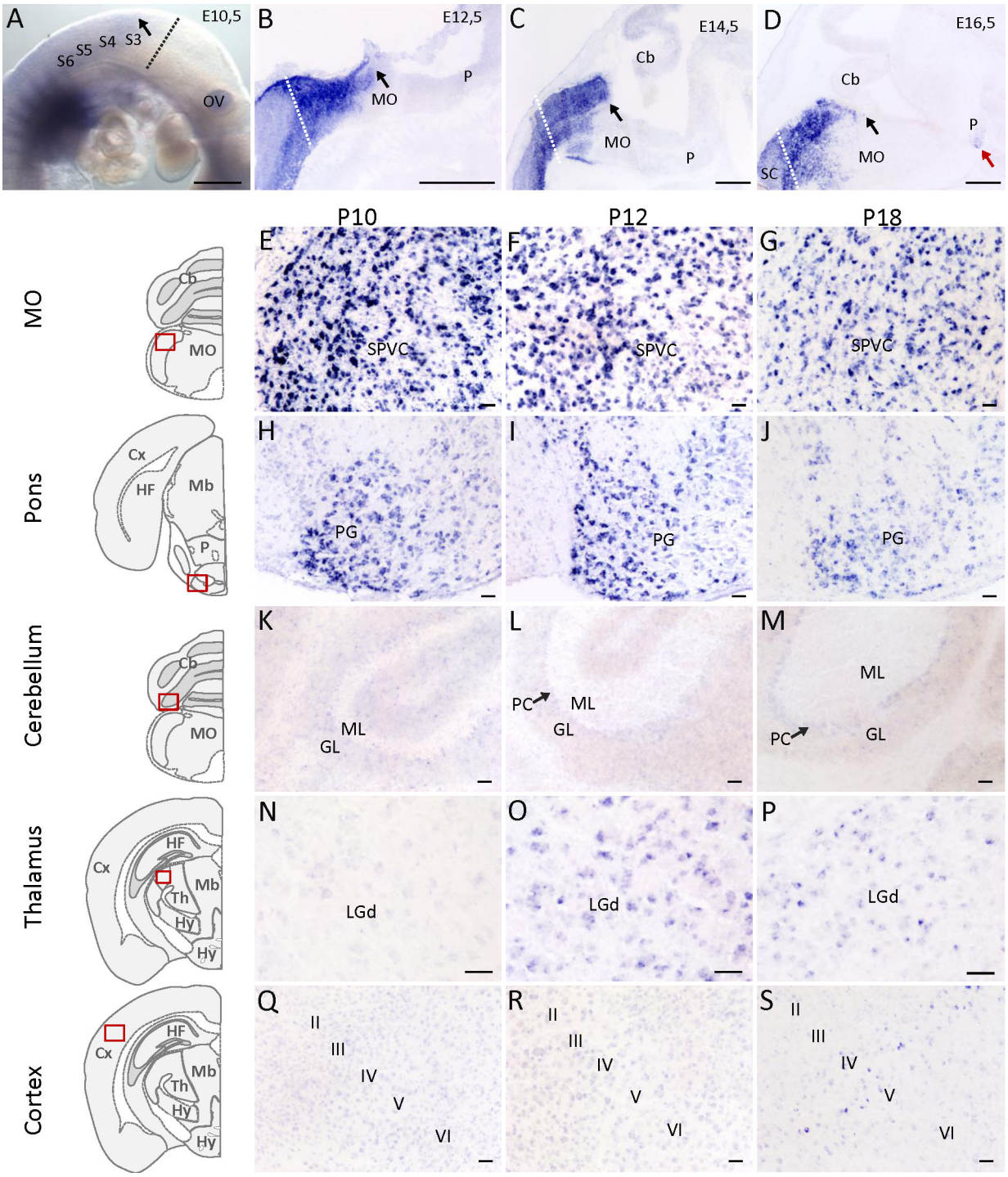

Figure 2. Dynamics of *Hoxa5* expression in the central nervous system at prenatal and postnatal stages. **A**: Whole-mount in situ hybridization (ISH) of embryo at E10.5. *Hoxa5* is expressed in the neural tube with an anterior limit of expression facing the somite 3 (black arrow). **B**–**D**: ISH of *Hoxa5* on sagittal cryosections of fetuses at E12.5, E14.5, and E16.5. *Hoxa5* is detected in the spinal cord (SC) and in the posterior part of the medulla oblongata (MO) at all stages (black arrows), while an additional expression domain is detected in the pons (P) only at E16.5 (red arrow). Dotted lines indicate the presumptive SC/brain boundary. **E**–**S**: ISH of *Hoxa5* on coronal cryosections of mouse brains at postnatal days P10, P12, and P18. Schematic views of coronal brain sections on the left side indicate the localization within the brain, with square red boxes referring to the localization of the pictures. At P10 (E,H,K,N,Q), a signal was present in the MO and P, but no signal was detected in the cerebellum (Cb), thalamus (Th), or cortex (Cx). At P12 (F,I,L,O,R), a signal was present in the MO, P, and Th, but no signal was detected in the Cb and Cx. At P18 (G,J,M,P,S), a signal was observed in the MO, P, Th, and cortex, while no signal was detected in the Cb. Medial is on the right, and lateral is on the left for E–S. For abbreviations, see list. Scale bar = 500 μm in A,C,D; 100 μm in B,E–S. [Color figure can be viewed at wileyonlinelibrary.com]

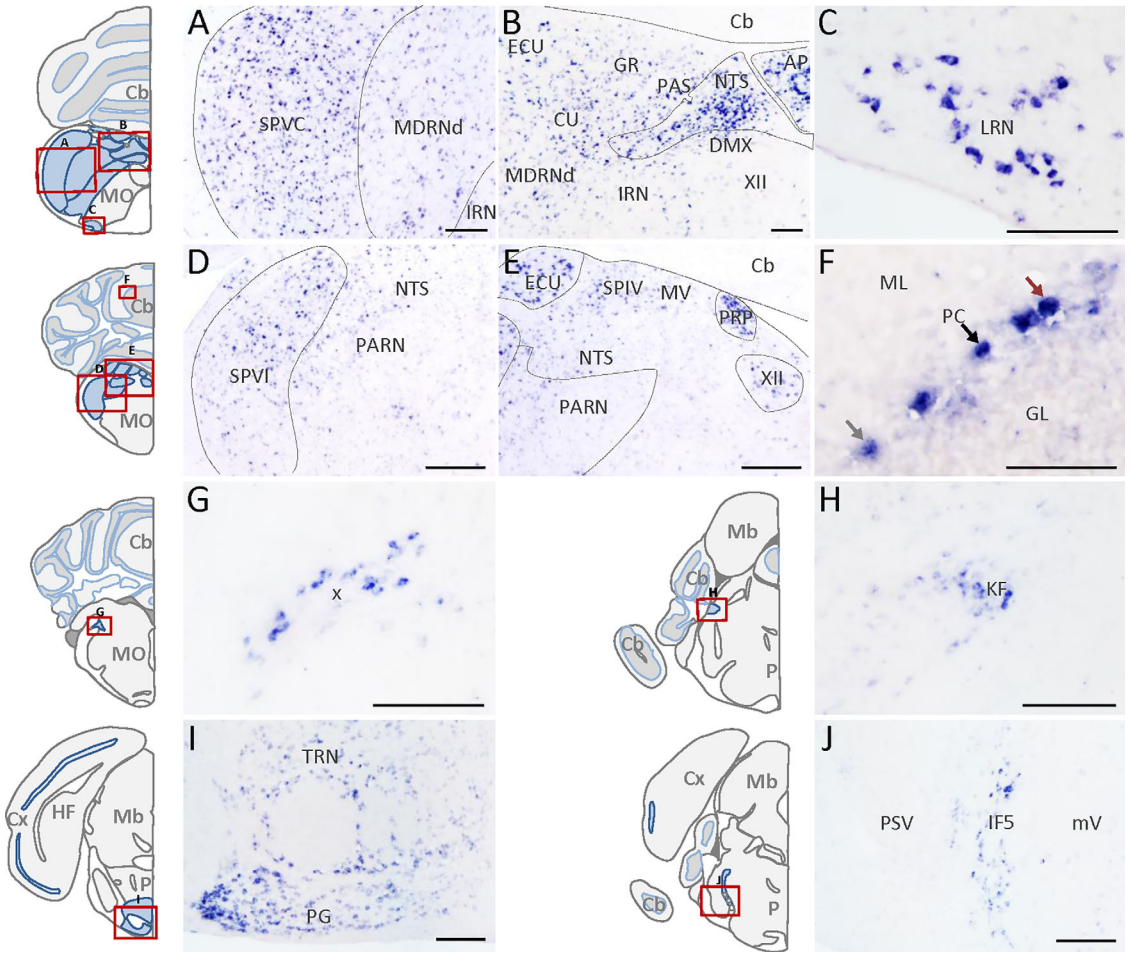

Figure 3. *Hoxa5* expression in the hindbrain of adult mice analyzed by in situ hybridization on coronal cryosections. Schematic views of coronal brain sections indicate the localization within the brain and areas with *Hoxa5* signal are highlighted by the blue color. Square red boxes on the schemes refer to the localization of the pictures. **A**: Expression in caudal part of the spinal nucleus of the trigeminal and dorsal part of the medullary reticular nucleus. **B**: Expression in the external cuneate nucleus, cuneate nucleus, gracile nucleus, nucleus of the solitary tract, parasolitary nucleus, dorsal motor nucleus of the vagus nerve, area postrema and intermediate reticular nucleus. **C**: Expression in the lateral reticular nucleus. **D**: Expression in the interpolar part of the spinal nucleus of the trigeminal and parvicellular reticular nucleus. **E**: Expression in the spinal vestibular nucleus, nucleus of the solitary tract, medial vestibular nucleus, nucleus prepositus, and anterior part of the hypoglossal nucleus. **F**: Expression in some Purkinje cells. Red arrow shows high-intensity signal in Purkinje cell, while gray arrow points to low-intensity signal. **G**: Expression in nucleus x. **H**: Expression in the Kölliker–Fuse subnucleus. **I**: Expression in the tegmental reticular nucleus and pontine gray. **J**: Expression in the interfascicular trigeminal nucleus. Medial is on the right, and lateral is on the left. For abbreviations, see list. Scale bar = 100 μm in A–E,G–J; 50 μm in F. [Color figure can be viewed at wileyonlinelibrary.com]

subnucleus (KF; Fig. 3H), which are "minor" precerebellar nuclei that have a less prominent projection to the cerebellum. Within the SPV, many cells are *Hoxa5* positive, suggesting that *Hoxa5* transcripts are also present in neurons that are not projecting to the cerebellum. Although it is not included in the precerebellar nuclei, we also detected *Hoxa5* labeling in the parasolitary nucleus (PAS; Fig. 3B). Neurons of the PAS relay vestibular signals to the inferior olive, the principal precerebellar nucleus that gives rise to climbing fibers, which synapse directly to dendrites of Purkinje cells. These signals provide information about spatial orientation along the longitudinal axis (Barmack and Yakhnitsa, 2000).

Finally, we also detected signal in the cerebellum at adulthood. It was of note that labeling was detected only in 10 cerebella out of the 19 brains analyzed by ISH, and with a different intensity of signal between brains. These observations could either suggest interindividual variation in expression or reflect the sensitivity threshold of ISH in territories of low gene expression. In cerebella where detectable signal was observed, it was always restricted to Purkinje cells, and was never detected reproducibly in other cerebellar layers or in deep cerebellar nuclei. Within Purkinje cells, the signal was variable between neighboring cells, giving a patchy appearance to the labeling (Fig. 3F). We observed this

TABLE 3.

Profile of *Hoxa5* Transcripts and HOXA5 Protein in the Medulla Oblongata and Pons Nuclei at Adulthood

		Main functions	Transcripts and protein
Medulla oblongata	XII (Hypoglossal nucleus)	MCNN	R
	X (Nucleus x)	mPN	H
	SPIV (Spinal vestibular nucleus)	mPN	R-S
	MV (Medial vestibular nucleus)	mPN	R-S
	PRP (Nucleus prepositus)	MPN	R-S
	PAS (Parasolitary nucleus)	ANS	H
	PARN (Parvicellular reticular nucleus)	mPN	R-S
	MDRN (Medullary reticular nucleus)	mPN	R-S
	IRN (Intermediate reticular nucleus)	mPN	R-S
	GRN (Gigantocellular reticular nucleus)	mPN	R-S
	DMX (Dorsal motor nucleus of the vagus nerve)	ANS- MCNN	R
	LRN (Lateral reticular nucleus)	MPN	H
	SPVI (Spinal nucleus of the trigeminal, interpolar part)	mPN- SCNN	R-S
	SPVC (Spinal nucleus of the trigeminal, caudal part)	mPN- SCNN	H
	NTS (Nucleus of the solitary tract)	mPN- ANS	H
	ECU (External cuneate nucleus)	MPN	H
	GR (Gracile nucleus)	ANS	S
	CU (Cuneate nucleus)	mPN	S
	AP (Area postrema)	ANS	H
Pons	IF5 (Interfascicular trigeminal nucleus)	MPN	H
	TRN (Tegmental reticular nucleus)	MPN	R
	PG (Pontine gray)	MPN	R
	KF (Kölliker–Fuse subnucleus)	mPN	R-S

Abbreviations: H, homogenous expression; R, regionalized expression; S, scattered expression; mPN, minor precerebellar nucleus; MPN, major precerebellar nucleus; ANS, autonomic nervous system; MCNN, motor cranial nerve nucleus; SCNN, sensory cranial nerve nucleus.

patchy appearance throughout the cerebellar cortex, and no relationship to lobular organization or band pattern could be established. Purkinje cells are central to the neuronal machinery of the cerebellum, receiving and integrating inputs from parallel fibers and climbing fibers, to provide information to the deep cerebellar nuclei, the sole output of the cerebellum (Sillitoe and Joyner, 2007).

Apart from the precerebellar system and cerebellum, we detected *Hoxa5* labeling in different nuclei implicated in the control of autonomic functions. The AP and the nucleus of the solitary tract (NTS) are two nuclei where *Hoxa5* transcripts were highly detected (Fig. 3B). These two nuclei are involved in the control of physiological functions including food intake and the cardiovascular system. The NTS is also implicated in gustatory processing, being the first central relay in the taste pathway (Norgren and Leonard, 1971; Norgren, 1978; Travers, 1988; Whitehead, 1990). We also detected signal in the dorsal part of the dorsal motor nucleus of the vagus nerve (DMX; Fig. 3B), which is involved in the control of food intake (Williams et al., 2000; Zhang et al., 2013) and in gastric function (Washabau et al., 1995; Krowicki et al., 2002). Finally, we detected *Hoxa5* labeling in the gracile nucleus (GR) as well as in its counterpart in the somatosensory system, the cuneate nucleus, carrying proprioceptive and touch sensation from the upper and lower body, respectively (Fig. 3B).

Forebrain

In continuity with the postnatal pattern, we detected signal in the thalamus and cerebral cortex in adulthood (Fig. 4). With respect to the cerebellum, we detected signal above background level in only a subset of brains (12 out of 19), but in expressing brains, the signal was always observed in both the thalamus and the cortex. The intensity of the hybridization signal in these two regions was also variable from one brain to another, reflecting either a biological variation between individuals or the limit of ISH sensitivity.

In the neocortex we detected *Hoxa5* labeling in a narrow layer of cells located in the medial region of sensory areas (visual, auditory, somatosensory; Fig. 4A), which are characterized by the presence of a prominent granular layer IV. In contrast, we did not observe labeling in the motor cortex or in the agranular cortices. The morphological features of labeled cells (pyramidal cell morphology) and their location (at the ventral border of layer IV) suggest that the signal is present in neurons of layer Va. To confirm this hypothesis, we performed double ISH with *Cux2*, a marker of cortical layers II–IV (Zimmer et al., 2004); and *Plxnd1*, a marker of layers II–Va (Watakabe et al., 2006). Comparison of *Hoxa5*

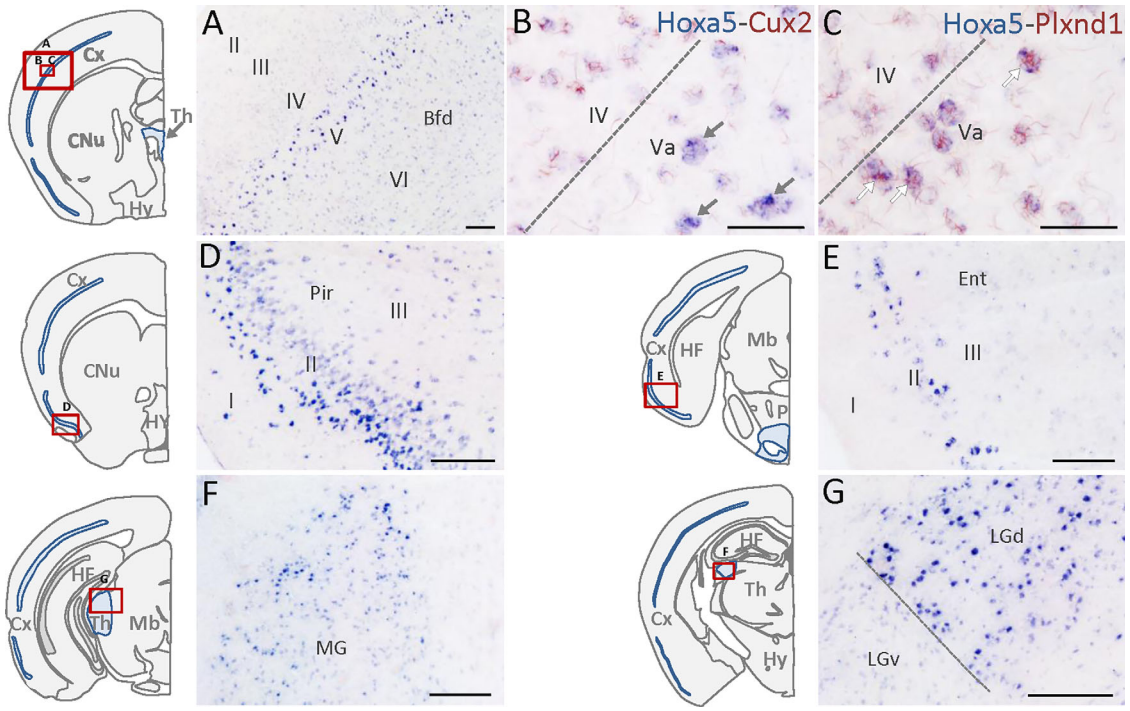

Figure 4. *Hoxa5* expression in the forebrain of adult mice analyzed by single in situ hybridization (ISH) (**A,D–G**) and double ISH with *Cux2* and *Plxnd1* (**B,C**) on coronal cryosections. Schematic views of coronal forebrain sections indicate the localization within the brain, and areas with *Hoxa5* signal are highlighted in blue. Square red boxes on the schemes refer to the localization of the pictures. A: In the barrel-field cortex, blue labeled cells were observed in a stripe of cells located medially between cortical layer IV and layer V. B: *Hoxa5* (blue labeling, gray arrows) show no colabeling with *Cux2* (red labeling) expressed in the layer IV of the somatosensory cortex. C: *Hoxa5* (blue labeling) and *Plxnd1* (red labeling) show a partly overlapping pattern in layer Va of the somatosensory cortex (white arrows). D: Signal was observed in the external part of layer II of the piriform area. E: Signal was observed in layer II of the lateral part of the entorhinal area. F: In the most posterior region of the thalamus (Th), the medial geniculate complex was labeled. G: In the posterior Th, signal was observed in the dorsal part of the lateral geniculate complex but not in the ventral part of the lateral geniculate complex. Medial is on the right, and lateral is on the left. For abbreviations, see list. Scale bar = 100 μm in A,D–G; 50 μm in B,C. [Color figure can be viewed at wileyonlinelibrary.com]

and *Cux2* signals showed that *Hoxa5*-positive cells are located close to the ventral border of *Cux2* labeling but without any colocalization of the two signals (Fig. 4B). However, double ISH for detection of *Hoxa5* and *Plxnd1* revealed colocalization of the two signals, confirming that *Hoxa5* transcripts are present in layer Va of the sensory cortices (Fig. 4C). In addition to the sensory cortex, we detected labeling in the piriform cortex, which is the primary olfactory cortex (Fig. 4D), and in the entorhinal cortex (Fig. 4E), the interface between the hippocampus and neocortex. In these areas the ISH signal was also restricted to a specific strip of cells located in layer IIa.

We also detected *Hoxa5* signal in 25 nuclei of the thalamus (Table 4). The major role of the thalamus is to gate and otherwise modulate the flow of information to the cortex, thus providing the most significant subcortical input to the neocortex (Jones, 1998). We paid particular attention to the sensory relays projecting to the neocortex areas in which we detected *Hoxa5* transcripts. In the auditory system, we detected labeling in the dorsal, medial, and ventral divisions of the medial geniculate complex (MG; Fig. 4F). Concerning the visual system, we detected signal in the dorsal lateral geniculate nucleus (LGd; Fig. 4G). In the somatosensory system, ISH signal was detected in the ventral posterior nucleus (VP) and the posterior nucleus (PO). In all the nuclei in which we detected *Hoxa5* signal, labeling appeared scattered.

Members of the *Hox* paralogy group tend to share broadly similar expression and regulation. Notably, *Hoxa5* and *Hoxb5* share a similar expression profile and induction pattern in the rostral CNS during development (Oosterveen et al., 2003, 2004; Ahn et al., 2014). We previously showed that *Hoxb5* is highly expressed in the hindbrain, but not in the anterior territories (Hutlet et al., 2014). To evaluate the singularity of *Hoxa5* expression in anterior territories and to complete the

TABLE 4.

Expression of *Hoxa5* in the Major Thalamic Nuclei at Adulthood

			Expression
Sensory-motor cortex related	Ventral group	VAL (Ventral anterior–lateral complex)	R
		VM (Ventral medial nucleus)	R
		VPL (Ventral posterolateral nucleus)	R
		VPLpc (Ventral posterolateral, parvicellular part)	R
		VPM (Ventral posteromedial nucleus)	R
		VPMpc (Ventral posteromedial nucleus, parvicellular part)	H
	Geniculate group, dorsal thalamus	MGd (Medial geniculate complex, dorsal part)	H
		MGv (Medial geniculate complex, ventral part)	H
		MGm (Medial geniculate complex, medial part)	H
		LGd (lateral geniculate, dorsal part)	H
Polymodal association cortex related	Lateral group	LP (Lateral posterior nucleus)	R
		PO (Posterior complex)	H
		POL (Posterior limiting nucleus)	R
		SGN (Suprageniculate nucleus)	H
	Anterior group	AV (Anteroventral nucleus)	H
		AMd (Anteromedial nucleus, dorsal part)	H
		AMv (Anteromedial nucleus, ventral part)	H
		IAM (interanteromedial nucleus)	R
	Medial group	IMD (Intermediodorsal nucleus)	R
		MDc (Mediodorsal nucleus, central part)	H
		MDl (Mediodorsal nucleus, lateral part)	H
		MDm (Mediodorsal nucleus, medial part)	H
		SMT (Submedial nucleus)	H
		PR (Perireunensis nucleus)	H
	Midline group	PVT (Paraventricular nucleus)	R
		PT (Parataenial nucleus)	R
	Intralaminar nuclei	RH (Rhomboid nucleus)	R
		CM (Central medial nucleus)	R
		PCN (Paracentral nucleus)	R
		CL (Central lateral nucleus)	H

Abbreviations: H, homogenous expression; R, regionalized expression.

information regarding the PG5 *Hox* genes, we compared expression of all three PG5 genes on neighboring coronal sections of adult brain (Fig. 5). In the hindbrain, *Hoxa5* and *Hoxb5* expression domains were highly similar, while *Hoxc5* was expressed at a lower level and in a more restricted pattern (Fig. 5A–F). In contrast, only *Hoxa5* transcripts were detected in the cerebellum, thalamus, and cortex (Fig. 5G–O).

Localization of HOXA5 protein in the brain

The distribution of the HOXA5 protein among the different brain cell types was examined by IHC using specific anti-HOXA5 antibodies, which were validated by IHC on *Hoxa5* KO tissues (Fig. 1).

Single labeling on adult brain sections at stages identical to those used for ISH analyses revealed HOXA5 signal in all nuclei of the medulla oblongata and the pons where transcripts were detected. In the 23 nuclei expressing *Hoxa5*, the presence of the protein was observed in the same pattern as described for the transcripts, either homogenous, restricted to a specific part of the nucleus, and/or scattered within nuclei cell populations (Table 3, Fig. 6A–F). In contrast, in the cerebellum, thalamus, and cortex no signal was detected by IHC in areas labeled with the *Hoxa5* probe corresponding to exon 1 as described above (Fig. 6G and data not shown). To increase the robustness of our data, two anti-HOXA5 antibodies were used that provided identical results. Next, double staining with antibodies directed to HOXA5 and NEUN, a marker of most neuronal cell types, was performed on hindbrain coronal sections (Fig. 7A–C). All the HOXA5-positive (HOXA5+) cells appeared to be NEUN+, suggesting that HOXA5 protein is present solely in neurons. Double IHC was next carried out with antibodies directed to the following glial markers: OLIG2 (Fig. 7D–F), a transcription factor expressed in oligodendrocyte nuclei, GFAP (Fig. 7G–I), specific to astrocytes, and MAC1 (CD11b/CD18; Fig. 7J–L), an integrin expressed by microglia. None of the glial markers tested colocalized with HOXA5, confirming that HOXA5 protein is present exclusively in neurons.

To identify the neuronal subpopulations in which HOXA5 is present, we performed double staining with

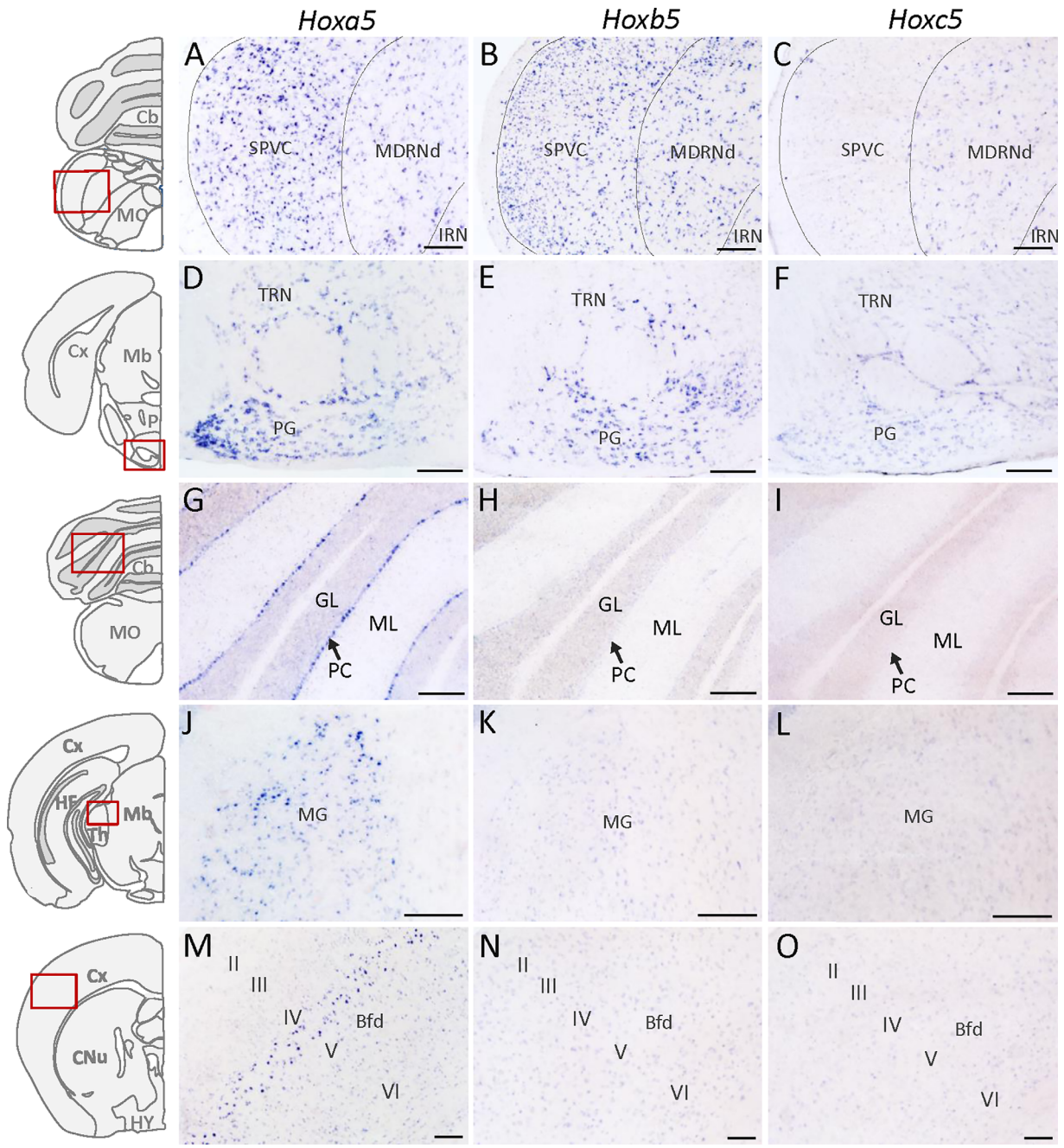

Figure 5. Comparative expressions of *Hoxa5, Hoxb5*, and *Hoxc5* in the adult brain analyzed by in situ hybridization on coronal cryosections. In the medulla oblongata (**A,B**) and the pons (**D,E**), a highly similar pattern was observed for *Hoxa5* and *Hoxb5*. In contrast, for *Hoxc5* only weak signal was detected in the medulla (**C**), and pons (**F**). In the cerebellum (**G–I**), the thalamus (**J–L**), and the cortex (**M–O**), labeling was detected only for *Hoxa5*. Medial is on the right, and lateral is on the left. For abbreviations, see list. Scale bar = 100 μm in A–O. [Color figure can be viewed at wileyonlinelibrary.com]

antibodies/probes directed to HOXA5 and to specific neuronal markers: ChAT for cholinergic neurons; TH for catecholaminergic neurons; VGLUT2 for glutamatergic neurons; and the two isoforms of glutamic acid decarboxylase (*Gad65* and *Gad67*) for GABAergic neurons. We did not observe any colocalization between HOXA5 and ChAT + cells, suggesting that HOXA5 is not present in cholinergic neurons (Fig. 7M–O). In contrast, in all the areas where HOXA5 was detected, HOXA5 + cells were also VGLUT2+, suggesting that HOXA5 is localized mainly in glutamatergic excitatory neurons (Fig. 7P–R). In a few nuclei, some HOXA5 + cells were TH + (Fig. 7S–U). Using ISH and IHC, we also observed colocalization between HOXA5 and the markers *Gad67*

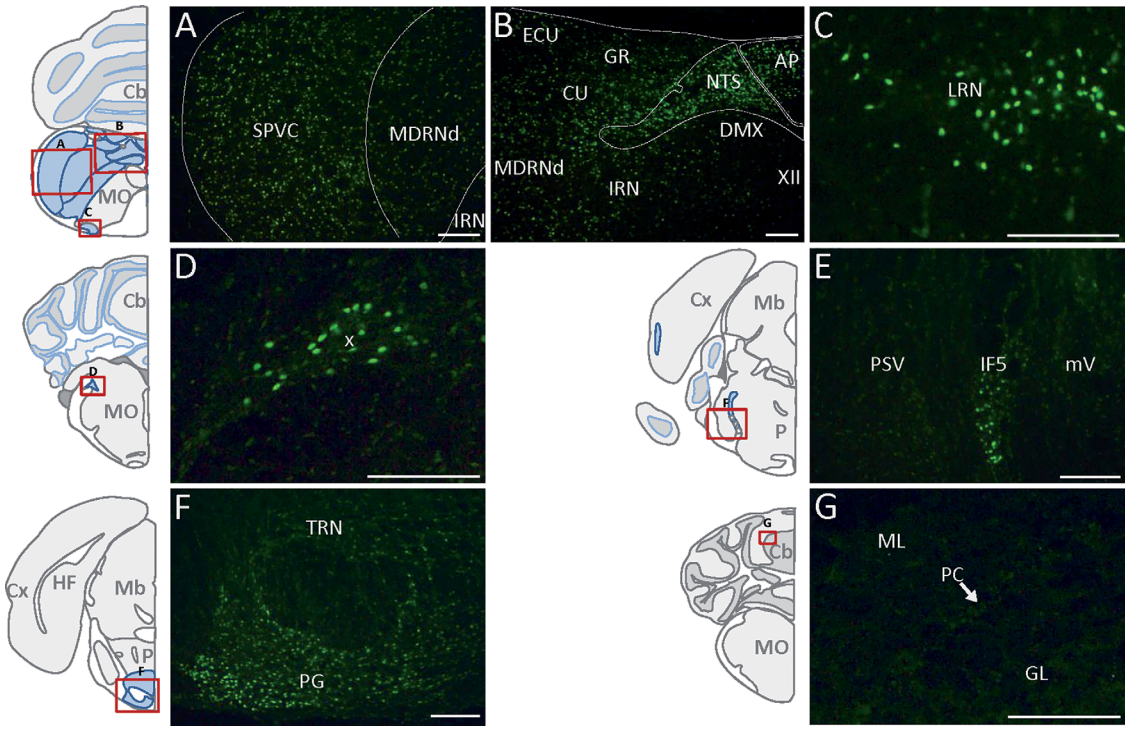

Figure 6. Anatomical localization of HOXA5 in the brain analyzed by immunolabeling of HOXA5 (green) on coronal cryosections. Schematic views of coronal brain sections indicate the localization within the brain, and areas with *Hoxa5* signal are highlighted in blue. Square red boxes on the schemes refer to the localization of the pictures. **A**: HOXA5 labeling in the caudal part of the spinal nucleus of the trigeminal and dorsal part of the medullary reticular nucleus. **B**: HOXA5 labeling in the external cuneate nucleus, cuneate nucleus, gracile nucleus, nucleus of the solitary tract, parasolitary nucleus, dorsal motor nucleus of the vagus nerve, area postrema, and intermediate reticular nucleus. **C**: HOXA5 labeling in the lateral reticular nucleus. **D**: HOXA5 labeling in nucleus x. **E**: HOXA5 labeling in the interfascicular trigeminal nucleus. **F**: HOXA5 labeling in the tegmental reticular nucleus and pontine gray. **G**: HOXA5 labeling in the cerebellum. Medial is on the right, and lateral is on the left. For abbreviations, see list. Scale bar = 100 μm in A–F; 50 μm in G. [Color figure can be viewed at wileyonlinelibrary.com]

(Fig. 7V–X) and *Gad65* (data not shown) in the medulla oblongata and the pons, suggesting that HOXA5 is also present in some GABAergic inhibitory neurons.

Differences in transcripts and protein profiles

The difference observed between *Hoxa5* transcripts and HOXA5 protein patterns could be explained either by the presence of a low amount of protein that would be below the threshold of IHC sensitivity, or by the presence of only noncoding transcripts in the cerebellum, thalamus, and cortex. To provide additional information regarding this discrepancy, and to test the first hypothesis (lower sensitivity of the IHC procedure compared with the ISH), we used RT-qPCR and western blotting approaches. Based on the expression profile observed by ISH, adult brains ($n = 5$) were macrodissected to isolate areas where *Hoxa5* transcripts were detected (posterior medulla oblongata; pons; cerebellum; thalamus; lateroventral cortex) and areas without detectable signal (mesencephalon; dorsomedial cortex; ventral telencephalon) (Fig. 8A). Both transcripts and proteins were isolated from the same samples, allowing for direct comparison of transcripts and proteins in the same extracts. RT-qPCR analysis confirmed the presence and high abundance of *Hoxa5* transcripts in the posterior medulla oblongata (Fig. 8B). In the pons, transcripts were amplified in all samples, at an abundance of about 4% compared with the medulla oblongata. Even though transcripts were reproducibly amplified in some other brain regions, they were not detected in all brains and/or the threshold cycles for amplification were too high ($Ct > 33$) to allow a robust conclusion. Using the western blot procedure, we were able to detect the presence of a specific band migrating approximately at 45 kDa (Joksimovic et al., 2005) only in the posterior medulla oblongata, and not in the pons (Fig. 8C), in contrast to IHC. This suggests that, in the present context of detection of transcripts/proteins with highly restricted distribution in endogenous tissues, these procedures are less sensitive than ISH and IHC, despite accurate dissection aimed to enrich the

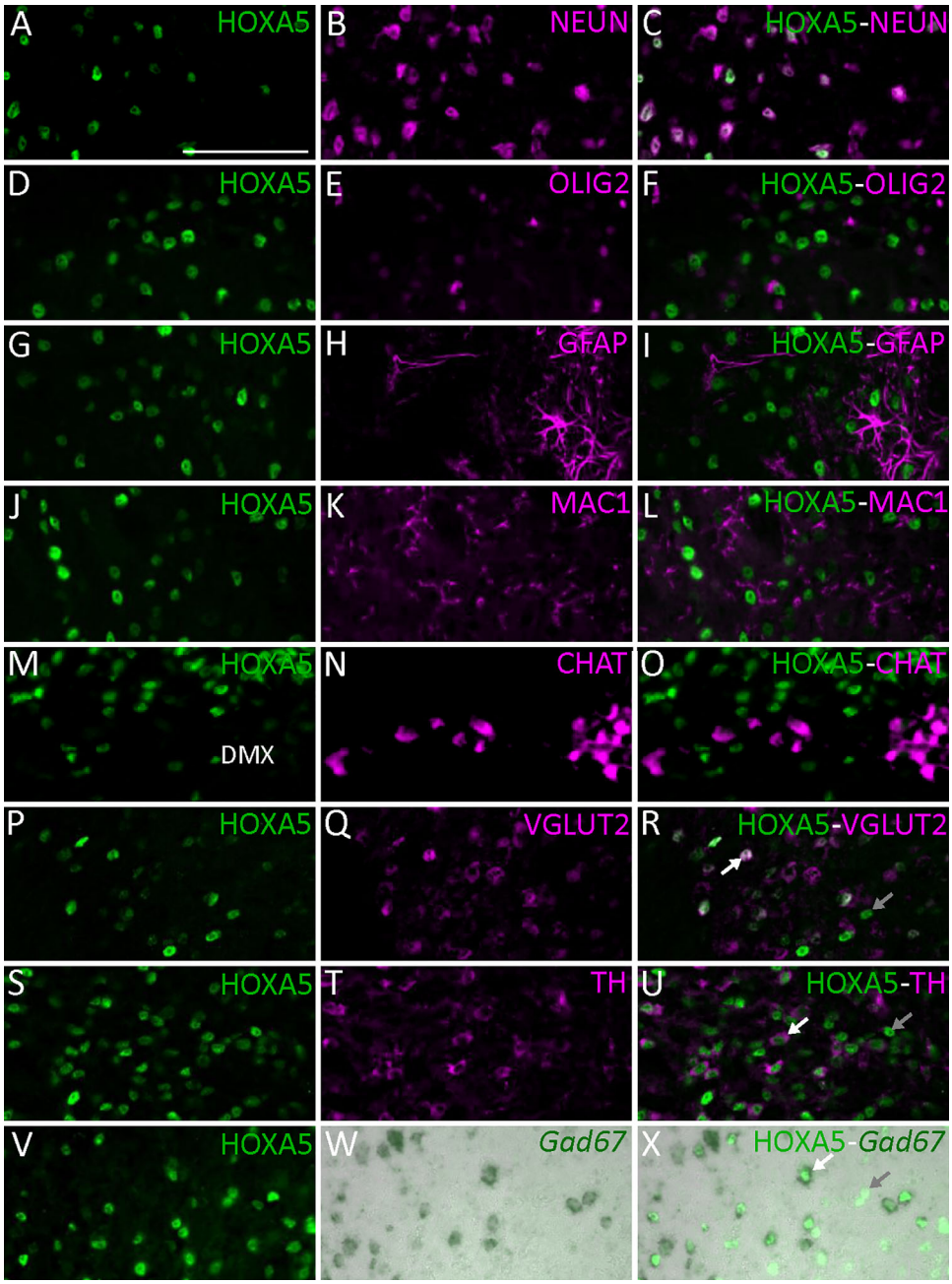

Figure 7. Cellular localization of HOXA5 in the brain analyzed by colabeling of HOXA5 (green) with neuronal, glial, and neuronal subpopulation markers (red and blue) on coronal cryosections of adult hindbrain. **A**–**C**: HOXA5-positive cells were detected in a fraction of neuronal cells that expressed NEUN. All the HOXA5-positive cells appeared to be NEUN positive (C). **D**–**L**: No colocalization was observed between HOXA5-positive cells and cells marked with OLIG2 expressed in oligodendrocytes (D–F), with GFAP expressed in astrocytes (G–I) and MAC1 expressed in microglia (J–L). **M**–**O**: HOXA5 was not detected in cholinergic neurons labeled with CHAT. **P**–**R**: In contrast, many HOXA5-positive cells were also VGLUT2-positive, identifying glutamatergic neurons. **S**–**U**: HOXA5 was present in the nuclei of a subset of catecholaminergic neurons labeled with TH. **V**–**X**: Immunolabeling of HOXA5 (green) on in situ hybridization labeling of the GABAergic marker *Gad67* (blue). HOXA5 protein was also detected in GABAergic neurons expressing *Gad67*. White arrows show examples of colocalization, while gray arrows show examples of cells only positive for HOXA5. For abbreviations, see list. Scale bar = 50 μm in A (applies to A–X). [Color figure can be viewed at wileyonlinelibrary.com]

samples in *Hoxa5* + cells. Technical limitations therefore prevent us at this stage from making conclusions as to the presence, or absence, of protein in anterior territories.

We next attempted to investigate the presence of noncoding transcripts in anterior areas. In embryonic tissues, multiple overlapping transcripts are produced from the *Hoxa5* transcriptional unit (Coulombe et al.,

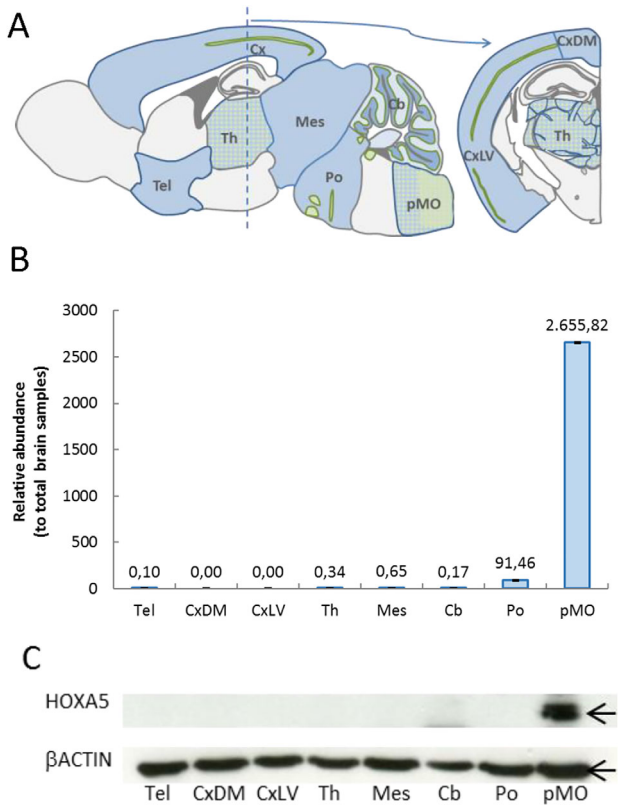

Figure 8. Hoxa5 transcripts and proteins analyzed in the adult brain by RT-qPCR and western blotting. **A**: Schematic representation of the eight regions macrodissected for analysis (posterior medulla oblongata [pMO]; pons [Po]; cerebellum [Cb]; mesencephalon [Mes]; thalamus [Th]; lateroventral cortex [CxLV]; dorsomedial cortex [CxDM]; ventral telencephalon [Tel]). Blue color represents dissected areas, while green color illustrates the *Hoxa5* expression pattern detected by in situ hybridization (homogenous or restricted/patchy). **B**: The RT-qPCR data are expressed according to the relative quantification of the ΔΔCt method, using *Hoxa5* expression in the whole brain as calibrator. Data are reported as means ± SEM, $n = 5$. Transcripts were reproducibly amplified only in the posterior medulla oblongata and in the pons. **C**: Western blot analysis using the rabbit anti-HOXA5 antibody. Aliquots (30 µg) of protein lysate were separated by SDS-PAGE and probed with anti-HOXA5 antibody. β-ACTIN detection was performed as loading control. A specific band migrating approximately at 45 kDa was detected only in the posterior medulla oblongata. [Color figure can be viewed at wileyonlinelibrary.com]

2010). Among the 1.8-, 5.0-, 9.5-, and 11.0-kb RNA species that have been described, all containing the HOXA5 open reading frame (ORF), only the shortest form would be translated into protein in vivo. Although we cannot distinguish all transcript variants, ISH was carried out on adult mouse brain cryosections using a probe corresponding to the *Hoxa5–Hoxa6* intergenic region recognizing only the longest transcripts (Probe b in Fig. 5 in Coulombe et al., 2010), and compared with signal observed with our probe corresponding to *Hoxa5* exon 1 and common to all transcripts (Fig. 9). Strikingly, the signal for the long transcripts appeared weak and less reproducible in the hindbrain nuclei where intense signal was observed with the exon 1 probe (Fig. 9A–D). In contrast, in the cerebellum, thalamus, and cortex, the signal observed was identical for both probes (Fig. 9E–J). Although we cannot exclude the presence of the shortest transcript in the forebrain and cerebellum, these results show that the signal observed in these territories is due, at least in part, to the presence of the larger, noncoding, transcripts.

DISCUSSION

In this study we characterized the expression profile and the neuroanatomical localization of *Hoxa5*/HOXA5 in the fetal, postnatal, and adult brain. At the RNA level, we showed that *Hoxa5* transcripts are present in the medulla oblongata and the pons from fetal to adult stages, and in the thalamus and the cortex from postnatal stages until adulthood (summarized in Fig. 10). We also showed that *Hoxa5* is transcribed in the adult cerebellum. At the protein level, we were able to detect HOXA5 solely in neurons of the hindbrain derivatives, mainly in glutamatergic and GABAergic neurons, as well as in some catecholaminergic neurons.

Dynamic expression of Hoxa5 in CNS development

The establishment and maintenance of *Hox* gene expression at gastrulation stages has been well described. While it has long been assumed that these patterns are maintained during later development, it has recently been shown that some undergo dynamic changes (Deschamps and van Nes, 2005; Ahn et al., 2014). In agreement with these data, we observed a rostral expansion of *Hoxa5* expression in the hindbrain between E10.5 and E12.5. Although the morphologic demarcations between rhombomeres are no longer visible at those late stages, the *Hoxa5* expression domain is clearly rostrally restricted to the caudalmost part of the hindbrain, likely corresponding to the enlarged embryonic r8. Based on the recently described segmental map of the fetal mouse medulla oblongata, *Hoxa5* expression could be more precisely located in the so-called crypto-rhombomeres r9–r11, with scattered cells in r8 (Tomas-Roca et al., 2014; see also Allen Developing Mouse Brain Reference Atlas; http://mouse.brain-map.org/static/atlas). This pattern also fits with the Hox mapping data reported by Tomas-Roca et al. (2014) at E14.5 and P0. As two conserved retinoic acid response elements (RAREs) have been identified within the *Hoxa* locus, one 5′ to *Hoxa4* and the other 3′ to

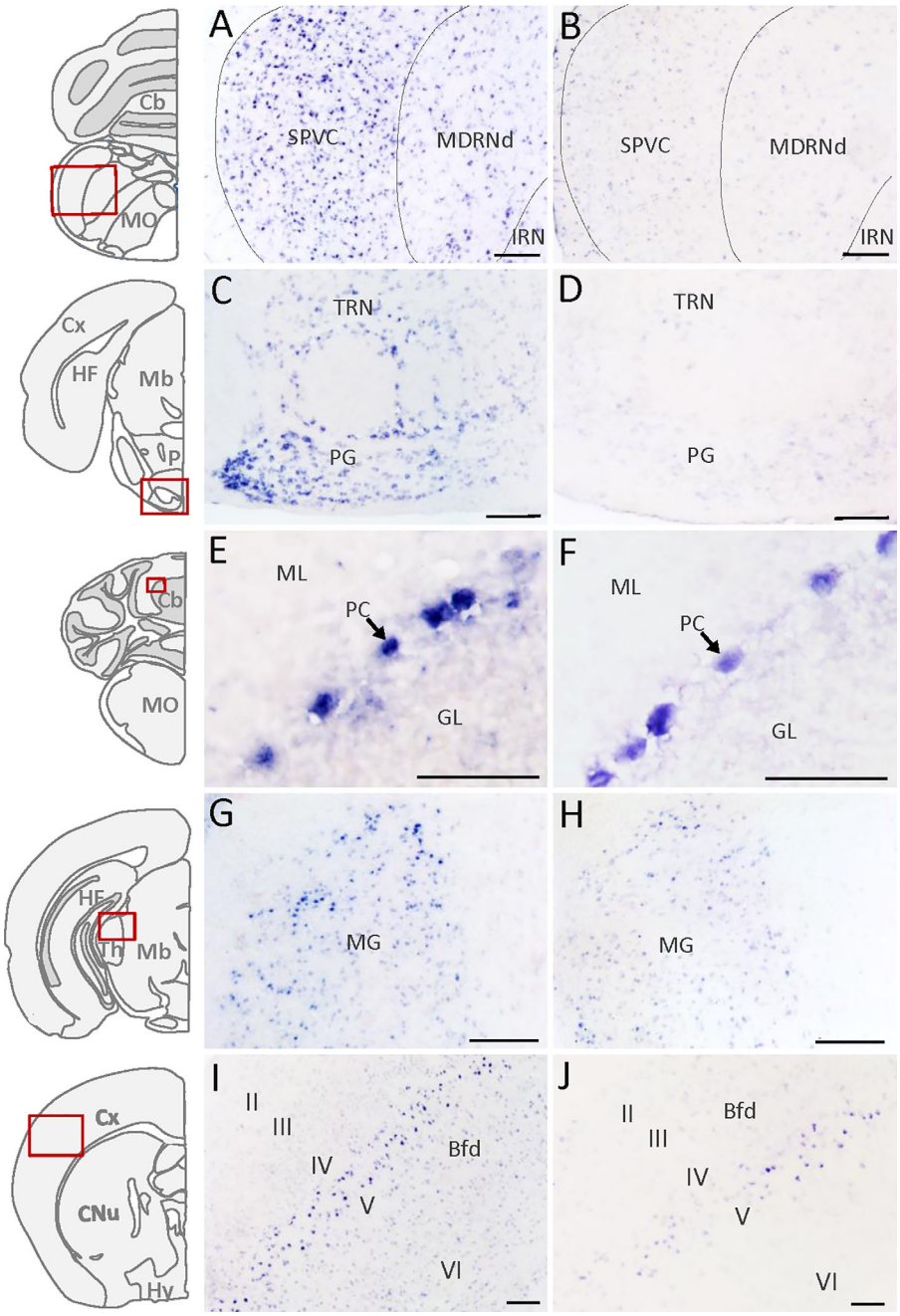

Figure 9. Differential expression of *Hoxa5* transcripts in the adult brain analyzed by in situ hybridization (ISH) on coronal cryosections. The middle column illustrates ISH labeling observed with a probe targeting sequences common to all transcripts described in Coulombe et al. (2010), while the right column illustrates labeling observed with a probe targeting only the larger (noncoding) transcripts of *Hoxa5*. In the medulla oblongata (**A,B**) and pons (**C,D**), no signal was observed with the probe targeting only the larger transcripts, in contrast to the probe targeting all transcripts. In the cerebellum (**E,F**), the thalamus (**G,H**), and the cortex (**I,J**), similar labeling was observed with both probes. Medial is on the right, and lateral is on the left. For abbreviations, see list. Scale bar = 100 μm in A–J. [Color figure can be viewed at wileyonlinelibrary.com]

Hoxa4, the *Hoxa5* rostral expansion could be regulated by retinoic acid signaling (Ahn et al., 2014). Such an actively regulated change in a *Hox* gene expression domain is not trivial and suggests a functional requirement at later developmental stages. Indeed, it has been shown that *Hoxa5*, together with other PG5 genes, is functionally involved in the tangential migration of pontine precerebellar neurons at fetal stages (Di Meglio et al., 2013). This is of particular interest, as we showed here that *Hoxa5* expression is enriched in precerebellar nuclei at adulthood.

Hoxa5 and the precerebellar circuits

During fetal development, lower rhombic lip progenitors undergo a long-distance migration to generate precerebellar nuclei. Progenitors from r6–r8 migrate through three different paths: the PG, TRN and the IF5 neurons take the anterior extramural migratory stream (AES) toward the pontine region, while the ECU and LRN neurons take the posterior extramural migratory stream (PES) toward the medulla region. The third stream is the intramural migratory stream (IMS), which gives rise to the inferior olive nuclei (Ray and Dymecki,

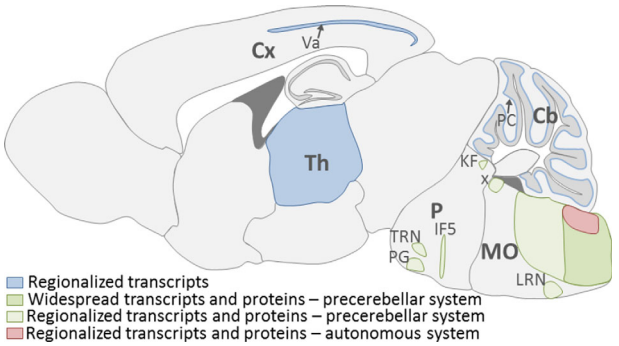

Figure 10. Summary of the *Hoxa5*/HOXA5 pattern in the adult mouse brain in a schematic view of a sagittal section. At the transcript level, *Hoxa5* was found to be expressed in the medulla oblongata (MO) and the pons from fetal to adult stages; in the thalamus and the cortex from postnatal stages until adulthood; and in the cerebellum at adulthood. At the protein level, HOXA5 was detected in neurons of the hindbrain derivatives in the precerebellar system (green labeling). In the caudal part of the medulla oblongata, HOXA5 localization was widespread (dark green), while in the anterior part it was restricted to a few nuclei (light green). HOXA5 was also detected in nuclei of the autonomic nervous system (red labeling). Blue labeling identifies brain regions where only transcripts were detected. For abbreviations, see list. [Color figure can be viewed at wileyonlinelibrary.com]

2009; Sotelo and Chédotal, 2013) In agreement with the presence of *Hoxa5* transcripts in the caudal rhombomeres, and hence in rhombic lip progenitors, we detected *Hoxa5* expression in the PG, TRN, IF5, ECU, and LRN from E14.5–E16.5 until later stages. We thus confirmed and extended previous data showing that *Hoxa5* expression is maintained in migrating and in settling precerebellar neurons in the AES and PES (Di Meglio et al., 2013). These authors also demonstrated that PG5 HOX proteins are functionally implicated in the topographic organization of migrating pontine neurons, notably through the negative regulation of *Unc5b* expression, a netrin repulsive receptor.

Once established, *Hoxa5* expression in the precerebellar neurons is maintained postnatally until adulthood. While most *Hox* mapping studies are based solely on transcript analysis, we show in the present study that the HOXA5 protein is present in all the *Hoxa5*-expressing hindbrain nuclei at adulthood. These data strengthen the idea that the activity of HOXA5 in these nuclei is required for processes beyond the patterning and neuronal migration phases. This could include axonal growth, pathfinding, and synapse formation during circuit establishment; refinement of neural circuits during early postnatal life in response to environmental cues; or adult synaptic plasticity. Although very few specific HOXA5 target genes have been identified, some support a role for HOXA5 in several of these processes.

Axonal growth relies on the interplay between environmental cues and their receptors belonging to the Ephrin/Eph, Slit/Robo, Netrin/Dcc-Unc families located on the growth cone. As mentioned above, *Unc5b* is a downstream target of HOX5 proteins (Di Meglio et al., 2013), and this regulation is required for topographic organization of migrating pontine neurons. After settling of the precerebellar neurons, HOXA5 could be involved in axonal growth and pathfinding of mossy fibers toward the developing cerebellum through a similar regulation. In support of the hypothesis of HOXA5 function in axonal growth, pleiotrophin (PTN), a heparin-binding growth factor, has been identified as a target of HOXA5 (Chen et al., 2005; Philippidou and Dasen, 2013). Several in vitro and in vivo studies have implicated PTN in the regulation of neurite outgrowth and guidance, as well as synaptogenesis (Li et al., 1990; Rauvala and Peng, 1997; Tanaka et al., 2003; Yanagisawa et al., 2010; Basille-Dugay et al., 2013). It is of note that, among the published downstream targets of HOXA5, Ephrin A1, Ephrin B2, and Akt (Rhoads et al., 2005; Arderiu et al., 2007) have also been implicated in cell migration and neuritogenesis (Read and Gorman, 2009). In addition to its neurite outgrowth-promoting activity, PTN has also been implicated in synaptic plasticity and learning in the hippocampus (Pavlov et al., 2002; del Olmo et al., 2009), and it has been suggested, based on its localization, that it could also participate in synaptic plasticity in the cerebellum (Basille-Dugay et al., 2013). Another target of HOXA5, the $G_{i/o}$ modulator L7/Pcp2, has also been implicated in synaptic plasticity (Sanlioglu et al., 1998; Redd et al., 2002; Iscru et al., 2009). *Pcp2* is highly abundant in cerebellar Purkinje cells, and its expression coincides with Purkinje cell development after birth. These data are particularly interesting as *Hoxa5* transcripts have also been detected in postnatal/adult Purkinje cells in this study and in a previous report (Sanlioglu et al., 1998).

In conclusion, based on the dynamic of *Hoxa5* expression and HOXA5 location, and in relation to the few identified targets, we can speculate that HOXA5 participates in the establishment and refinement/plasticity of precerebellar neuronal circuits during postnatal and adult life. Thus HOXA5 could influence adult cerebellar functions such as coordinated motor activity, motor learning, and procedural memory.

Hoxa5 and the autonomic system

We also detected both *Hoxa5* transcripts and HOXA5 protein in different nuclei involved in the control of autonomic functions: the AP and NTS, and the dorsal part of the DMX. These nuclei are implicated in the physiological control of food intake, gastric, respiratory,

and cardiovascular functions. For example, the NTS is implicated in gustatory processing (Norgren and Leonard, 1971; Norgren, 1978; Travers, 1988; Whitehead, 1990) and is the first central relay of lung and airway vagal afferents (Kubin et al., 2006). Strikingly, plasticity in the NTS has been highlighted in both the gustatory and respiratory systems (Bonham et al., 2006; Hill and May, 2007). It is thus tempting to speculate that, as in the precerebellar circuits, HOXA5 could be maintained in restricted brainstem neurons to control processes related to synaptic plasticity at postnatal and adult stages.

It is also worth mentioning that *Hoxa5*$^{-/-}$ mutant mice die perinatally due to respiratory failure that has been linked to defective development of the respiratory tract (Aubin et al., 1997). However, these authors also report impaired breathing, which could be related to recent data showing that absence of *Hox5* genes results in a severe defect in diaphragm innervation and an important reduction and disorganization of motoneurons in the phrenic motor column (Philippidou et al., 2012). In addition to the respiratory phenotype, the loss of *Hoxa5* causes a delay in acquisition of the adult mode of digestion that is normally coordinated with the process of spontaneous weaning (Aubin et al., 1999). These data, combined with our observations, suggest successive and multilevel functions of HOXA5 in respiratory and digestive tracts, and indicate that in addition to its role in patterning and organogenesis of these systems, HOXA5 could also coordinate their proper innervation prenatally and regulate their functions postnatally.

Hoxa5 and the forebrain

In the forebrain, a *Hoxa5* signal was detected no earlier than the second week of postnatal life. As cortical and thalamic neurons are born within these territories, these domains of expression cannot be explained by migration of progenitors expressing *Hoxa5* at embryonic/fetal stages, and suggest de novo transcription of the *Hoxa5* locus in these differentiated cells after birth.

In the neocortex, Hoxa5 expression was restricted to a narrow row of cells in the visual, auditory, and somatosensory cortices, in areas where layer IV is present. Double labeling allowed us to localize this expression to layer Va. This layer integrates information from layer IV and layer Va and would play a role in intracortical processing of sensory information (Schubert et al., 2006). In addition, a signal for *Hoxa5* was detected in a strip of cells at the external side of layer II in the entorhinal and piriform cortices.

In contrast to the brainstem, we did not detect the HOXA5 protein in the forebrain and the cerebellum. This difference between mRNA and protein distribution could be explained by a lower sensitivity of the IHC procedure with respect to the ISH. In that case, the HOXA5 protein would be produced, but in an amount too low to be detected by IHC. In an attempt to substantiate these data, we implemented more quantitative procedures, namely RT-qPCR and western blot, with the objective of detecting both transcripts and proteins in the same brain samples. Unfortunately, in the paradigm used here, the sensitivity of both procedures appeared to be lower than the qualitative detection. As the number of *Hoxa5* + cells is extremely low, especially in the anterior territories, the transcripts and proteins were probably too diluted in the macrodissected samples to be detected. As this approach did not allow us to circumvent the sensitivity problem, we cannot conclude at this stage whether the protein is present in a low amount or is not produced. Alternatively, it has been shown that multiple overlapping transcripts encompassing the *Hoxa5* coding sequence are produced in embryos. They arise from the use of distinct promoters and from alternative splicing of RNAs. Among the 1.8-, 5.0-, 9.5-, and 11.0-kb RNA species, only the shortest form would be translated into protein in vivo (Jeannotte et al., 1993; Coulombe et al., 2010); the other transcripts would be "noncoding." Differences in the expression profiles of these different transcripts have been reported (Larochelle et al., 1999; Coulombe et al., 2010). Using a probe allowing the detection of the longer transcripts but not the shortest one, we provided evidence that some of these transcripts are indeed present in the cerebellum, thalamus, and cortex.

Long noncoding RNAs (LncRNAs) have been the subject of intense research and debates in recent years, with potential implications for gene regulation. Notably, recent advances have revealed the presence of both sense and antisense noncoding sequences within the four *Hox* clusters (Mainguy et al., 2007; De Kumar and Krumlauf, 2016). Although their functions remain poorly understood, some of them could be associated with regulatory functions, both in *cis* or in *trans*, in *Hox* gene expression (Wang et al., 2011; reviewed by De Kumar and Krumlauf, 2016). Nevertheless, most of these LncRNAs are antisense and/or transcribed only from intergenic regions, and do not contain *Hox* coding sequences, in contrast to the larger transcripts variants described at the *Hoxa5* locus. Although it would be tempting to speculate that these transcripts are LncRNAs with potential regulatory functions, either on *Hoxa5* or neighboring *Hox* genes, it is much too early to discuss these issues.

Our results thus suggest that some of the previously described *Hoxa5* transcript variants are produced in the cortex and thalamus from postnatal stages until

adulthood, and in the cerebellum at adulthood. Data produced by IHC, RT-qPCR, and western blot analyses support the hypothesis that these variants are noncoding RNAs that are not translated into the HOXA5 protein. Although we cannot totally exclude the possibility that a protein is produced, it is likely that the only products generated in the anterior territories are *Hoxa5* transcripts. Whether these LncRNAs are functional, and whether these functions are associated with the *Hoxa5* gene or not, are appealing questions that remain to be addressed.

CONCLUSIONS

Our study has established the foundations for discovering new functions of *Hoxa5*/HOXA5 in the CNS. To address all of the functional hypotheses generated by this descriptive analysis, studies that identify the HOXA5 target genes in the postnatal brain are urgently required, as well as the development of conditional mutants that will allow evaluation of the consequences of late loss-of-function.

ACKNOWLEDGMENTS

The authors are very grateful to Coralie Piget for animal husbandry and Tom Van Acker for technical support. We wish to thank Lucie Jeannotte for providing the probe for ISH and *Hoxa5* KO samples for antibody validation. We also thank René Rezsöhazy and Bernard Knoops for helpful discussions and Helen Christian for critical reading of the manuscript.

CONFLICT OF INTEREST STATEMENT

The authors have no conflicts of interest associated with this work.

ROLE OF AUTHORS

All authors had full access to all of the data in the study and take responsibility for the integrity of the data and the accuracy of the data analysis. Study concept and design: BL, FG. Acquisition of data: BL, DB, DS, MH. Analysis and interpretation of data: BL, BH, FG. Drafting of the manuscript: BL, FG. Critical revision of the manuscript for important intellectual content: BL, BH, DB, FG. Approval of final manuscript draft: BL, BH, DB, DS, MH, MTA, FG. Obtained funding: BL, FG. Administrative, technical, and material support: MTA. Study supervision: FG.

LITERATURE CITED

Ahn Y, Mullan HE, Krumlauf R. 2014. Long-range regulation by shared retinoic acid response elements modulates dynamic expression of posterior Hoxb genes in CNS development. Dev Biol 388:134–144.

Arderiu G, Cuevas I, Chen A, Carrio M, East L, Boudreau NJ. 2007. HoxA5 stabilizes adherens junctions via increased Akt1. Cell Adh Migr 1:185–195.

Aubin J, Lemieux M, Tremblay M, Berard J, Jeannotte L. 1997. Early postnatal lethality in Hoxa-5 mutant mice is attributable to respiratory tract defects. Dev Biol 192:432–445.

Aubin J, Chailler P, Menard D, Jeannotte L. 1999. Loss of Hoxa5 gene function in mice perturbs intestinal maturation. Am J Physiol 277:C965–973.

Aubin J, Dery U, Lemieux M, Chailler P, Jeannotte L. 2002. Stomach regional specification requires Hoxa5-driven mesenchymal-epithelial signaling. Development 129: 4075–4087.

Barmack NH, Yakhnitsa V. 2000. Vestibular signals in the parasolitary nucleus. J Neurophysiol 83:3559–3569.

Basille-Dugay M, Hamza MM, Tassery C, Parent B, Raoult E, Benard M, Raisman-Vozari R, Vaudry D, Burel DC. 2013. Spatio-temporal characterization of the pleiotrophinergic system in mouse cerebellum: evidence for its key role during ontogenesis. Exp Neurol 247:537–551.

Bechara A, Laumonnerie C, Vilain N, Kratochwil CF, Cankovic V, Maiorano NA, Kirschmann MA, Ducret S, Rijli FM. 2015. Hoxa2 selects barrelette neuron identity and connectivity in the mouse somatosensory brainstem. Cell Rep 13:783–797.

Bonham AC, Chen CY, Sekizawa S, Joad JP. 2006. Plasticity in the nucleus tractus solitarius and its influence on lung and airway reflexes. J Appl Physiol 101:322–327.

Cavicchioli L, Flanigan TP, Dickson JG, Vantini G, Dal Toso R, Fusco M, Walsh FS, Leon A. 1991. Choline acetyltransferase messenger RNA expression in developing and adult rat brain: regulation by nerve growth factor. Brain Res Mol Brain Res 9:319–325.

Chen H, Rubin E, Zhang H, Chung S, Jie CC, Garrett E, Biswal S, Sukumar S. 2005. Identification of transcriptional targets of HOXA5. J Biol Chem 280:19373–19380.

Chotteau-Lelievre A, Dolle P, Gofflot F. 2006. Expression analysis of murine genes using in situ hybridization with radioactive and nonradioactively labeled RNA probes. Methods Mol Biol 326:61–87.

Colberg-Poley AM, Voss SD, Chowdhury K, Stewart CL, Wagner EF, Gruss P. 1985. Clustered homeo boxes are differentially expressed during murine development. Cell 43:39–45.

Coulombe Y, Lemieux M, Moreau J, Aubin J, Joksimovic M, Berube-Simard FA, Tabaries S, Boucherat O, Guillou F, Larochelle C, Tuggle CK, Jeannotte L. 2010. Multiple promoters and alternative splicing: Hoxa5 transcriptional complexity in the mouse embryo. PLoS One 5:e10600.

Dasen JS, Jessell TM. 2009. Hox networks and the origins of motor neuron diversity. Curr Top Dev Biol 88:169–200.

De Kumar B, Krumlauf R. 2016. HOXs and lincRNAs: Two sides of the same coin. Science Adv 2:e1501402.

del Olmo N, Gramage E, Alguacil LF, Perez-Pinera P, Deuel TF, Herradon G. 2009. Pleiotrophin inhibits hippocampal long-term potentiation: a role of pleiotrophin in learning and memory. Growth Factors 27:189–194.

Deschamps J, van Nes J. 2005. Developmental regulation of the Hox genes during axial morphogenesis in the mouse. Development 132:2931–2942.

Di Bonito M, Glover JC, Studer M. 2013a. Hox genes and region-specific sensorimotor circuit formation in the hindbrain and spinal cord. Dev Dyn 242:1348–1368.

Di Bonito M, Narita Y, Avallone B, Sequino L, Mancuso M, Andolfi G, Franze AM, Puelles L, Rijli FM, Studer M. 2013b. Assembly of the auditory circuitry by a Hox genetic network in the mouse brainstem. PLoS Genet 9: e1003249.

Di Meglio T, Kratochwil CF, Vilain N, Loche A, Vitobello A, Yonehara K, Hrycaj SM, Roska B, Peters AH, Eichmann A, Wellik D, Ducret S, Rijli FM. 2013. Ezh2 orchestrates topographic migration and connectivity of mouse precerebellar neurons. Science 339:204–207.

Fu Y, Tvrdik P, Makki N, Machold R, Paxinos G, Watson C. 2013. The interfascicular trigeminal nucleus: a precerebellar nucleus in the mouse defined by retrograde neuronal tracing and genetic fate mapping. J Comp Neurol 521:697–708.

Geisen MJ, Di Meglio T, Pasqualetti M, Ducret S, Brunet JF, Chedotal A, Rijli FM. 2008. Hox paralog group 2 genes control the migration of mouse pontine neurons through slit-robo signaling. PLoS Biol 6:e142.

Goemaere J, Knoops B. 2012. Peroxiredoxin distribution in the mouse brain with emphasis on neuronal populations affected in neurodegenerative disorders. J Comp Neurol 520:258–280.

Hill DL, May OL. 2007. Development and plasticity of the gustatory portion of nucleus of the solitary tract. In: Bradley RM, editor. The role of the nucleus of the solitary tract in gustatory processing. Boca Raton, FL: CRC Press/Taylor & Francis.

Hutlet B, Theys N, Coste C, Ahn MT, Doshishti-Agolli K, Lizen B, Gofflot F. 2014. Systematic expression analysis of Hox genes at adulthood reveals original patterns in the central nervous system. Brain Struct Funct 221:1223–1243.

Iscru E, Serinagaoglu Y, Schilling K, Tian J, Bowers-Kidder SL, Zhang R, Morgan JI, DeVries AC, Nelson RJ, Zhu MX, Oberdick J. 2009. Sensorimotor enhancement in mouse mutants lacking the Purkinje cell-specific Gi/o modulator, Pcp2(L7). Mol Cell Neurosci 40:62–75.

Jeannotte L, Lemieux M, Charron J, Poirier F, Robertson EJ. 1993. Specification of axial identity in the mouse: role of the Hoxa-5 (Hox1.3) gene. Genes Dev 7:2085–2096.

Joksimovic M, Jeannotte L, Tuggle CK. 2005. Dynamic expression of murine HOXA5 protein in the central nervous system. Gene Expr Patterns 5:792–800.

Jones EG. 1998. Viewpoint: the core and matrix of thalamic organization. Neuroscience 85:331–345.

Krowicki ZK, Burmeister MA, Berthoud HR, Scullion RT, Fuchs K, Hornby PJ. 2002. Orexins in rat dorsal motor nucleus of the vagus potently stimulate gastric motor function. Am J Physiol Gastrointest Liver Physiol 283:G465–472.

Krumlauf R, Holland PW, McVey JH, Hogan BL. 1987. Developmental and spatial patterns of expression of the mouse homeobox gene, Hox 2.1. Development 99:603–617.

Kubin L, Alheid GF, Zuperku EJ, McCrimmon DR. 2006. Central pathways of pulmonary and lower airway vagal afferents. J Appl Physiol 101:618–627.

Larochelle C, Tremblay M, Bernier D, Aubin J, Jeannotte L. 1999. Multiple cis-acting regulatory regions are required for restricted spatio-temporal Hoxa5 gene expression. Dev Dyn 214:127–140.

Lee VM, Page CD, Wu HL, Schlaepfer WW. 1984. Monoclonal antibodies to gel-excised glial filament protein and their reactivities with other intermediate filament proteins. J Neurochem 42:25–32.

Li YS, Milner PG, Chauhan AK, Watson MA, Hoffman RM, Kodner CM, Milbrandt J, Deuel TF. 1990. Cloning and expression of a developmentally regulated protein that induces mitogenic and neurite outgrowth activity. Science 250:1690–1694.

Mainguy G, Koster J, Woltering J, Jansen H, Durston A. 2007. Extensive polycistronism and antisense transcription in the mammalian Hox clusters. PLoS One 2:e356.

Mallo M, Wellik DM, Deschamps J. 2010. Hox genes and regional patterning of the vertebrate body plan. Dev Biol 344:7–15.

Masserano JM, Weiner N. 1983. Tyrosine hydroxylase regulation in the central nervous system. Mol Cell Biochem 53–54:129–152.

Mullen RJ, Buck CR, Smith AM. 1992. NeuN, a neuronal specific nuclear protein in vertebrates. Development 116: 201–211.

Narita Y, Rijli FM. 2009. Hox genes in neural patterning and circuit formation in the mouse hindbrain. Curr Top Dev Biol 88:139–167.

Nolte C, Krumlauf R. 2007. Expression of Hox genes in the nervous system of vertebrates. In: Papageorgio S, editor. HOX gene expression. New York, NY: Landes Bioscience and Springer Science+Business Media. p 14–41.

Norgren R. 1978. Projections from the nucleus of the solitary tract in the rat. Neuroscience 3:207–218.

Norgren R, Leonard CM. 1971. Taste pathways in rat brainstem. Science 173:1136–1139.

Oosterveen T, Niederreither K, Dolle P, Chambon P, Meijlink F, Deschamps J. 2003. Retinoids regulate the anterior expression boundaries of 5′ Hoxb genes in posterior hindbrain. EMBO J 22:262–269.

Oosterveen T, Meijlink F, Deschamps J. 2004. Expression of retinaldehyde dehydrogenase II and sequential activation of 5′ Hoxb genes in the mouse caudal hindbrain. Gene Expr Patterns 4:243–247.

Oury F, Murakami Y, Renaud JS, Pasqualetti M, Charnay P, Ren SY, Rijli FM. 2006. Hoxa2- and rhombomere-dependent development of the mouse facial somatosensory map. Science 313:1408–1413.

Pasqualetti M, Diaz C, Renaud JS, Rijli FM, Glover JC. 2007. Fate-mapping the mammalian hindbrain: segmental origins of vestibular projection neurons assessed using rhombomere-specific Hoxa2 enhancer elements in the mouse embryo. J Neurosci 27:9670–9681.

Pavlov I, Voikar V, Kaksonen M, Lauri SE, Hienola A, Taira T, Rauvala H. 2002. Role of heparin-binding growth-associated molecule (HB-GAM) in hippocampal LTP and spatial learning revealed by studies on overexpressing and knockout mice. Mol Cell Neurosci 20:330–342.

Philippidou P, Dasen JS. 2013. Hox genes: choreographers in neural development, architects of circuit organization. Neuron 80:12–34.

Philippidou P, Walsh CM, Aubin J, Jeannotte L, Dasen JS. 2012. Sustained Hox5 gene activity is required for respiratory motor neuron development. Nat Neurosci 15: 1636–1644.

Rauvala H, Peng HB. 1997. HB-GAM (heparin-binding growth-associated molecule) and heparin-type glycans in the development and plasticity of neuron-target contacts. Prog Neurobiol 52:127–144.

Ray RS, Dymecki SM. 2009. Rautenlippe redux—toward a unified view of the precerebellar rhombic lip. Curr Opin Cell Biol 21:741–747.

Read DE, Gorman AM. 2009. Involvement of Akt in neurite outgrowth. Cell Mol Life Sci 66:2975–2984.

Redd KJ, Oberdick J, McCoy J, Denker BM, Luo Y. 2002. Association and colocalization of G protein alpha subunits and Purkinje cell protein 2 (Pcp2) in mammalian cerebellum. J Neurosci Res 70:631–637.

Rezsohazy R, Saurin AJ, Maurel-Zaffran C, Graba Y. 2015. Cellular and molecular insights into Hox protein action. Development 142:1212–1227.

Rhoads K, Arderiu G, Charboneau A, Hansen SL, Hoffman W, Boudreau N. 2005. A role for Hox A5 in regulating angiogenesis and vascular patterning. Lymph Res Biol 3:240–252.

Rodriguez CI, Dymecki SM. 2000. Origin of the precerebellar system. Neuron 27:475–486.

Sanchez-Madrid F, Simon P, Thompson S, Springer TA. 1983. Mapping of antigenic and functional epitopes on the alpha- and beta-subunits of two related mouse glycoproteins involved in cell interactions, LFA-1 and Mac-1. J Exp Med 158:586–602.

Sanlioglu S, Zhang X, Baader SL, Oberdick J. 1998. Regulation of a Purkinje cell-specific promoter by homeodomain proteins: repression by engrailed-2 vs. synergistic activation by Hoxa5 and Hoxb7. J Neurobiol 36:559–571.

Schubert D, Kotter R, Luhmann HJ, Staiger JF. 2006. Morphology, electrophysiology and functional input connectivity of pyramidal neurons characterizes a genuine layer va in the primary somatosensory cortex. Cereb Cortex 16: 223–236.

Sillitoe RV, Joyner AL. 2007. Morphology, molecular codes, and circuitry produce the three-dimensional complexity of the cerebellum. Annu Rev Cell Dev Biol 23:549–577.

Sotelo C, Chédotal A. 2013. Hindrain tangential migration. In: Rubenstein J, Rakic P, editors. Cellular migration and formation of neuronal connections. Amsterdam: Elsevier. p 345–362.

Springer TA. 1981. Monoclonal antibody analysis of complex biological systems. Combination of cell hybridization and immunoadsorbents in a novel cascade procedure and its application to the macrophage cell surface. J Biol Chem 256:3833–3839.

Tanaka M, Maeda N, Noda M, Marunouchi T. 2003. A chondroitin sulfate proteoglycan PTPzeta /RPTPbeta regulates the morphogenesis of Purkinje cell dendrites in the developing cerebellum. J Neurosci 23:2804–2814.

Tomas-Roca L, Corral-San-Miguel R, Aroca P, Puelles L, Marin F. 2014. Crypto-rhombomeres of the mouse medulla oblongata, defined by molecular and morphological features. Brain Struct Funct 221:815–838.

Travers JB. 1988. Efferent projections from the anterior nucleus of the solitary tract of the hamster. Brain Res 457:1–11.

Vigneault E, Poirel O, Riad M, Prud'homme J, Dumas S, Turecki G, Fasano C, Mechawar N, El Mestikawy S. 2015. Distribution of vesicular glutamate transporters in the human brain. Front Neuroanat 9:23.

Wang KC, Yang YW, Liu B, Sanyal A, Corces-Zimmerman R, Chen Y, Lajoie BR, Protacio A, Flynn RA, Gupta RA, Wysocka J, Lei M, Dekker J, Helms JA, Chang HY. 2011. A long noncoding RNA maintains active chromatin to coordinate homeotic gene expression. Nature 472:120–124.

Washabau RJ, Fudge M, Price WJ, Barone FC. 1995. GABA receptors in the dorsal motor nucleus of the vagus influence feline lower esophageal sphincter and gastric function. Brain Res Bull 38:587–594.

Watakabe A, Ohsawa S, Hashikawa T, Yamamori T. 2006. Binding and complementary expression patterns of semaphorin 3E and plexin D1 in the mature neocortices of mice and monkeys. J Comp Neurol 499:258–273.

Whitehead MC. 1990. Subdivisions and neuron types of the nucleus of the solitary tract that project to the parabrachial nucleus in the hamster. J Comp Neurol 301:554–574.

Williams DL, Kaplan JM, Grill HJ. 2000. The role of the dorsal vagal complex and the vagus nerve in feeding effects of melanocortin-3/4 receptor stimulation. Endocrinology 141:1332–1337.

Yanagisawa H, Komuta Y, Kawano H, Toyoda M, Sango K. 2010. Pleiotrophin induces neurite outgrowth and up-regulates growth-associated protein (GAP)-43 mRNA through the ALK/GSK3beta/beta-catenin signaling in developing mouse neurons. Neuroscience Res 66:111–116.

Zhang W, Zhang C, Fritze D, Chai B, Li J, Mulholland MW. 2013. Modulation of food intake by mTOR signalling in the dorsal motor nucleus of the vagus in male rats: focus on ghrelin and nesfatin-1. Exp Physiol 98:1696–1704.

Zhou Q, Wang S, Anderson DJ. 2000. Identification of a novel family of oligodendrocyte lineage-specific basic helix-loop-helix transcription factors. Neuron 25:331–343.

Zimmer C, Tiveron MC, Bodmer R, Cremer H. 2004. Dynamics of Cux2 expression suggests that an early pool of SVZ precursors is fated to become upper cortical layer neurons. Cereb Cortex 14:1408–1420.